Electronic Supplementary Material (ESI) for Journal of Materials Chemistry C.
This journal is © The Royal Society of Chemistry 2019

Supporting Information

Smart, chiral, and non-conjugated cyclohexane-based bis-salicylaldehyde hydrazides: multi-stimuli-responsive, turn-on, ratiometric, and thermochromic fluorescence, single crystal structures, and DFT calculations

Man Wang‡[a], Caiqi Cheng‡[b,c] Li Chunbo,[a] Dehua Wu,[a] Jintong Song,[a] Jun Wang,[b] Xiangge Zhou,[a] Haifeng Xiang[a], and Jin Liu*[c]*

[a] *College of Chemistry, Sichuan University, Chengdu, 610041, China. Fax: (+86) 28-8541-2291. *E-mail: xianghaifeng@scu.edu.cn.*

[b] *State Key Laboratory of Oral Diseases, Department of Orthodontics, West China Hospital of Stomatology, Sichuan University, Chendu, Sichuan, China.*

[c] *Laboratory of Stem Cell Biology, State Key Laboratory of Biotherapy, West China Hospital, Sichuan University, Chengdu, 610064, China. *E-mail: ljamelia@163.com.*

‡ These authors contributed equally to this work.

Experimental Section

Materials and Instrumentation. All reagents were purchased from commercial suppliers and used without further purification. All the Salen ligands were prepared according to previous reports.[14] ^{1}HNMR (400MHz) spectra were recorded in DMSO-d_6. Chemical shifts are reported in ppm using tetramethylsilane as internal standard. UV/vis absorption spectra were recorded using a U5100 (Hitachi) spectrophotometer with quartz cuvettes of 1 cm pathlength. Fluorescence spectra were obtained using F-7000 Fluorescence spectrophotometer (Hitachi) at room temperature. The slit width was 5 nm and 2.5 nm for excitation and emission. The photon multiplier voltage was 400 V. CD spectra were recorded using a Chirascan plus qCD (Applied Photophysics) at room temperature. Samples in solution and powder were contained in 1 cm path length quartz cuvettes (3.5 mL volume) and quartz tube, respectively. Emission decay lifetime experiments were performed by Horiba Tempro-01 (Horiba Scientific). C, H, and N element analyses were performed by employing Flash1112 elemental analyzers (Thermo Fisher Scientific). CD spectra were recorded using a Chirascan plus qCD (Applied Photophysics) at room temperature. Samples in solution and powder were contained in 1 cm path length quartz cuvettes (3.5 mL volume) and quartz tube, respectively.

Measurement of Fluorescence Quantum Yield (Φ). The quantum yield of a solution sample was measured by the optical dilute method of Demas and Crosby with a standard of quinine sulfate (Φ_r = 0.55, quinine in 0.05 mol dm^{-3} sulfuric acid) calculated by: $\Phi_s = \Phi_r(B_r/B_s)(n_s/n_r)^2(D_s/D_r)$, where the subscripts s and r refer to the sample and reference standard solution respectively; *n* is the refractive index of the solvents; D is the integrated intensity. The excitation intensity *B* is calculated by: $B = 1 - 10^{-AL}$, where A is the absorbance at the excitation wavelength and L is the optical path length (L = 1 cm in all cases). The refractive indices of the solvents at room temperature are taken from standard source.

X-ray Crystallographic Analysis. The determination of the unit cell and data collection for four single crystal samples were performed on a Xcalibur E X-ray single crystal diffractometer equipped with graphite monochromator Mo Kα (λ=0.71073 Å) radiation. The data collection was executed using CrysAlisPro program. Structures were solved by direct method and successive Fourier difference syntheses (SHELXS-97), and were refined by full matrix least-squares procedure on F2 with anisotropic thermal parameters for all nonhydrogen atoms (SHELXL-97).

Computational Details. Calculations were carried out using the Gaussian 09 software package [B3LYP 6-31G(d,p)] based on the X-ray single-crystal structures. The ground state

geometry was optimized using DFT and excited states were predicted using the ground state geometry using TD-DFT, from where UV/Vis absorption and CD spectra (pcm method for solvent effect; 50 singlet−singlet transitions) were predicted.

Cell Culture Methods and Imaging. The imaging of The human gastric cancer cell lines (IM95m) was finished by Fluorescence Vertical Microscope-Zeiss AX10 imager A2/AX10 cam HRC. The human gastric cancer cell lines (IM95m), purchased from JCRB Cell Bank (NIBIO, Osaka, Japan), was cultured in Modified PRMI Medium (Hyclone, Utah, USA) supplemented with 10% fetal bovine serum (Gibco, California, USA), 100 U/ml penicillin and 100 ug/ml streptomycin (Hyclone, Utah, USA) at 37 °C in an atmosphere containing 5.0 % CO_2. Cells were routinely grown in 100-mm plastic tissue culture dishes (Corning, New York, USA) and harvested using a 0.25 % Trypsin-EDTA solution (Corning, New York, USA) when they reached the logarithmic growth phase. Cells were maintained in these culture conditions for all experiments. After removing the incubating media and rinse with PBS for three times, the cells were incubated with the dye (1.0×10^{-5} mol dm^{-3}) in PBS for 2 h at room temperature. Then, the cells were washed three times with PBS and incubated with aqueous alkali for 15 min. At last, the cells were imaged with confocal microscope.

Cytotoxicity studies: To evaluate the toxicity of the fluorescent dyes, Cell Counting Kit-8 (CCK-8 assay, Sigma, St. Louis, MO, USA) was used to assess the living cells viability. The more toxic the fluorescent dyes are, the less viability the cells have. Modified PRMI media with different dyes (1.0×10^{-5} mol dm^{-3}) were added into each well, after the cells are seeded at a density of 2000 per well in the 96-well plate. Thereafter, the CCK-8 assay was used on 0 h, 12 h, 24 h, 48 h and the OD value was measured by BioTek ELX800 (Bio-Tek, Winooski, VT, USA) at the wavelength of 450 nm.

Measurement of ion probes: Anion titration experiment was started with the dye (10 mL) of known concentration (1.0×10^{-5} mol dm^{-3} in DMSO/DMF/EtOH). For the titration, various metal ions and anions (1.0–0.10 mol dm^{-3} sodium or potassium salts in water) were added by a microsyringe. All types of absorption and fluorescence measurement were monitored at about 1 hours after the addition of the ion to the dye solution at room temperature.

Measurement of amino acid and diamine probes: Diamine titration experiment was started with the dye (10 mL) of known concentration (1.0×10^{-5} mol dm^{-3} in DMSO). For the titration, various *D*- or *L*-amino acids (1.0×10^{-2}–1.0×10^{-1} mol dm^{-3} in water) and chiral diamine (1.0×10^{-2}–1.0×10^{-1} mol dm^{-3} in DMSO) were added by a microsyringe.

All types of absorption and fluorescence measurement were monitored at about 2 hours after the addition of the anion to the dye solution at room temperature.

Synthesis of Organic Dyes: **Cy-bis-SHs** were prepared by a similar method (Fig. 3) according to previous reports.[31,53]

(*R,R*)/(*S,S*) methyl cyclohexanedicarboxylic acid **(2)**: (*R,R*)/(*S,S*) cyclohexanedicarboxylic acid **(1)** (3.44 g, 20 mmol) was added into a 50 ml round-bottom flask with 30 ml MeOH. Under stirring in ice-water bath, $SOCl_2$ (3 ml, 40 mmol) was carefully dropped, and then the resulted solution was stirred overnight at room temperature. The the solvent of final solution was removed by rotary evaporator to obtain colorless oily liquid, which need not purify further for the next prepartion step (Yield 80 %).

(*R,R*)/(*S,S*) cyclohexanedicarboxylic hydrazide **(3)**: (*R,R*)/(*S,S*) methyl cyclohexanedicarboxylate **(2)** (1.6 g) was added in a 50 ml round-bottom flask with 25 ml MeOH. 80% hydrazine hydrate (1.6 ml) was added and then stirred at 40 °C for 24 hours. The resuted suspension solution was filtrated and washed with MeOH and ether in turn to get white powder (Yield 56 %).

Cy-bis-SHs were prepared by a similar method. The mixture of salicyaldehyde or salicylaldehyde derivatives (2.0 mmol) and (*R,R*)/(*S,S*) cyclohexanedicarboxylic hydrazide **(3)** (1.0 mmol) in 30 mL EtOH solution was refluxed at 78 °C for 5-6 h. After the reaction was complete, the mixture was cooled to room temperature and then the product in crystal or powder was collected by filtration.

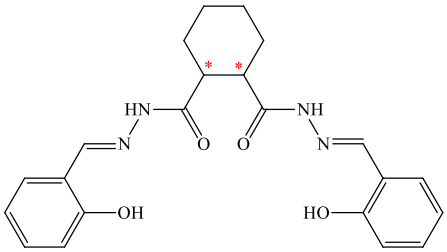

(*R,R*)/(*S,S*)-H (Yield 70 %): ^{1}H NMR (400 MHz, DMSO) δ 11.78 (s, 1H), 11.14 (s, 1H), 8.35 (s, 1H), 7.49 (d, *J* = 8.0 Hz, 1H), 7.26 (s, 1H), 6.90 (s, 2H), 2.66 – 2.61 (m, 1H), 1.87 (d, *J* = 48.8 Hz, 2H), 1.37 – 1.30 (m, 2H).^{13}C NMR (101 MHz, DMSO) δ 171.06, 157.86, 147.02, 131.61, 130.02, 119.72, 119.07, 116.76, 44.41, 30.01, 25.50. HRMS (ESI): Calculated for $C_{22}H_{24}N_4O_4$ [[M+Na]$^+$] 431.4478, found 431.4470. Anal. Calcd. (Found): C, 64.69 (64.69); H, 5.92 (5.91); N, 13.72 (13.72).

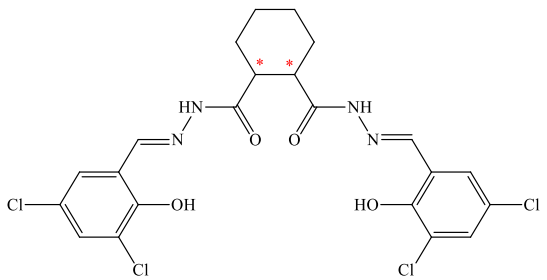

(*R*,*R*)/(*S*,*S*)-3,5-Cl (Yield 65 %): ^{1}H NMR (400 MHz, DMSO) δ 12.29 (s, 1H), 12.18 (s, 1H), 8.32 (s, 1H), 7.63 (s, 1H), 7.58 (s, 1H), 2.67 (s, 1H), 1.89 (d, *J* = 59.5 Hz, 2H), 1.34 (s, 2H). ^{13}C NMR (101 MHz, DMSO) δ 171.37, 152.53, 146.01, 130.49, 128.79, 123.28, 121.77, 121.16, 44.37, 29.83, 25.41. HRMS (ESI): Calculated for $C_{22}H_{20}Cl_4N_4O_4$ [[M+Na]$^+$] 567.1036, found 567.1035. Anal. Calcd. (Found): C, 48.38 (48.39); H, 3.69 (3.69); N, 10.26 (10.25).

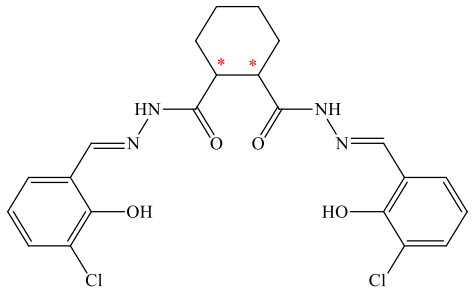

(*S*,*S*)/(*R*,*R*)-3-Cl (Yield 78 %): ^{1}H NMR (400 MHz, DMSO) δ 12.22 (s, 1H), 12.04 (s, 1H), 8.35 (d, *J* = 2.7 Hz, 1H), 7.46 – 7.42 (m, 2H), 6.93 (t, *J* = 7.8 Hz, 1H), 2.67 (d, *J* = 9.4 Hz, 1H), 1.90 (dd, *J* = 62.8, 8.9 Hz, 2H), 1.43 – 1.31 (m, 2H). ^{13}C NMR (101 MHz, DMSO) δ 171.22, 153.54, 147.49, 131.57, 129.81, 120.67, 120.37, 120.04, 44.36, 29.91, 25.66, 25.44. HRMS (ESI): Calculated for $C_{22}H_{22}Cl_2N_4O_4$ [[M+Na]$^+$] 499.0916, found 499.0917, Anal. Calcd. (Found): C, 55.36 (55.37); H, 4.65 (4.66); N, 11.74 (11.73).

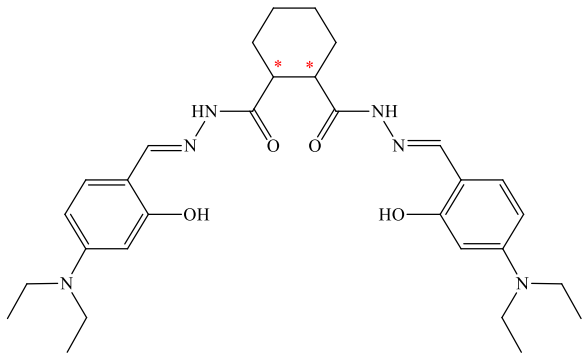

(*S*,*S*)/(*R*,*R*)-4-NEt$_2$ (Yield 75 %)**:** ^{1}H NMR (400 MHz, DMSO) δ 11.40 (s, 1H), 11.29 (s, 1H), 8.12 (s, 1H), 7.13 (d, *J* = 8.7 Hz, 1H), 6.22 (t, *J* = 8.9 Hz, 1H), 6.08 (t, *J* = 3.8 Hz, 1H), 3.32 (d, *J* = 6.9 Hz, 4H), 2.61 – 2.53 (m, 1H), 1.84 (dd, *J* = 46.6, 8.2 Hz, 2H), 1.32 (dd, *J* = 19.2, 9.8 Hz, 2H), 1.10 – 1.06 (m, 6H). ^{13}C NMR (101 MHz, DMSO) δ 170.03, 159.97, 150.39, 148.65, 131.92, 106.58, 103.92, 97.89, 44.39, 44.21, 30.13, 25.48, 13.00. HRMS (ESI):

Calculated for $C_{30}H_{42}N_6O_4$ [[M+Na]$^+$] 573.3165, found 573.3162. Anal. Calcd. (Found): C, 65.43 (65.42); H, 7.69 (7.69); N, 15.26 (15.25).

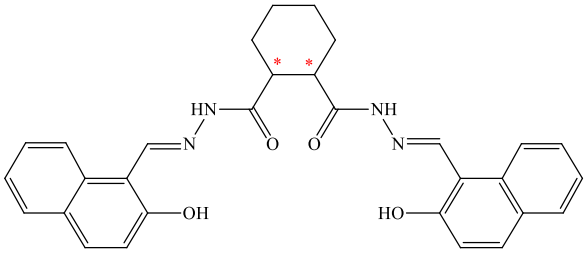

(*S*,*S*)/(*R*,*R*)-NaPh (Yield 70 %)**:** ^{1}H NMR (400 MHz, $CDCl_3$) δ 11.90 (s, 1H), 11.13 (s, 1H), 9.20 (s, 1H), 8.22 (d, *J* = 8.5 Hz, 1H), 7.90 (dd, *J* = 8.4, 5.3 Hz, 3H), 7.61 (d, *J* = 5.1 Hz, 1H), 7.42 (d, *J* = 7.0 Hz, 1H), 7.19 (d, *J* = 9.0 Hz, 1H), 2.76 – 2.68 (m, 1H), 2.05 – 1.87 (m, 2H), 1.48 – 1.38 (m, 2H). ^{13}C NMR (101 MHz, DMSO) δ 170.83, 158.21, 145.53, 132.94, 131.95, 129.37, 128.25, 128.16, 123.93, 121.16, 119.27, 108.94, 44.57, 30.02, 25.50. HRMS (ESI): Calculated for $C_9H_{10}N_2O_2$ [[M+Na]$^+$] 531.2008, found 531.2010. Anal. Calcd. (Found): C, 70.85 (70.86); H, 5.55 (5.54); N, 11.02 (11.01).

Table. S1 Photophysical data of **Cy-bis-SHs** at room temperature.

	medium	λ_{abs}/nm (ε/dm^3 mol^{-1}cm^{-1})	λ_{em}/nm	Stokes shift/nm	Φ
(*R*,*R*)/(*S*,*S*)-H	Toluene	282(8.26×10^4); 326(1.88×10^4)	466	140	0.011
	DCM	280(2.46×10^4); 289(2.37×10^4); 322(1.18×10^4)	495	173	0.013
	THF	277(3.75×10^4); 281(4.44×10^4); 321(1.85×10^4)	481	160	0.11
	MeCN	280(9.53×10^4); 320(4.42×10^4)	482	162	0.014
	DMF	280(5,27×10^4); 321(3.17×10^4) 389(3.50×10^3)	478	89	0.31
	DMSO	282(6,27×10^4); 325(4.59×10^4)	477	152	0.11
	MeOH	277(9.63×10^4); 322(4.72×10^4)	478	156	0.11
	Solid		no emission		
(*R*,*R*)/(*S*,*S*)-3-Cl	Toluene	284(5.18×10^4);324(3.68×10^4)	457	133	0.006
	DCM	281(4.07×10^4) 320(1.29×10^4)	470	150	0.008
	THF	280(2.67×10^4) 321(1.09×10^3)	477	156	0.085
	MeCN	283(4.50×10^4);322(1.74×10^4)	485	163	0.0049
	DMF	286(3.75×10^4); 323(1.74×10^4)	478	155	0.31
	DMSO	289(3.53×10^4); 323(1.31×10^4)	476	156	0.054
	MeOH	286(2.86×10^4); 321(1.94×10^4)	480	159	0.19
	EtOH	283(1.56×10^4); 323(1.51×10^4); 379(5.3×10^3)	481	158	0.045
	Solid		no emission		
(*R*,*R*)/(*S*,*S*)-3,5-Cl	Toluene	287(4.86×10^4); 332(2.07×10^4); 411(1.09×10^3)	557	146	0.003
	DCM	287(4.57×10^4); 332(2.67×10^4); 411(3.14×10^3)	552	141	0.002
	THF	287(3.07×10^4); 330(2.43×10^4); 410(1.06×10^3)	484	74	0.101
	MeCN	282(6.22×10^4); 333(2.11×10^4); 400(3.52×10^3)	463	51	0.012
	DMF	286(2.84×10^4); 333(1.04×10^4); 411(5.8×10^3)	490	79	0.012
	DMSO	285(4.29×10^4); 331(1.7×10^4); 411(4.60×10^3)	441	30	0.004
	MeOH	287(3.29×10^4); 332(1.73×10^4); 412(3.26×10^3)	4882	76	0.15

	EtOH	283(1.29×10^4); 330(1.93×10^4) 411(1.16×10^3)	486	75	0.18
	Solid		no emission		
(*R*,*R*)/(*S*,*S*)-4-NEt$_2$	Toluene	357(2.61×10^4);	no emission		
	DCM	360(7.38×10^4);			
	THF	357(2.68×10^4);			
	MeCN	353(6.94×10^4);			
	DMF	355(7.71×10^4);			
	DMSO	355(8.82×10^4);			
	MeOH	350(2.43×10^4);			
	EtOH	357(6.33×10^4);			
	Solid				
(*R*,*R*)/(*S*,*S*)-Naph	Toluene	321(3.28×10^4); 354(2.79×10^4)	no emission		
	DCM	322(1.75×10^4); 355(1.54×10^4)			
	THF	321(4.28×10^4); 354(2.99×10^4)			
	MeCN	321(1.99×10^4); 355(1.45×10^4)			
	DMF	322(3.01×10^4); 355(2.41×10^4); 427(5.70×10^3)			
	DMSO	321(5.34×10^4); 359(4.44×10^4); 408(2.39×10^3)			
	MeOH	321(2.50×10^4); 355(3.09×10^4)			
	EtOH	321(4.28×10^4); 353(3.27×10^4)			
	Solid		no emission		

Table. S2 Calculated results of **(*S*,*S*)-3-Cl** for mechanism of polar solvent-induced fluorescence.

		λ_{abs}/nm	f_{osc}	
Method 1	Excited State 1	321.83	0.2203	HOMO−3→LUMO 4.41% HOMO−1→LUMO 74.55% HOMO→LUMO+1 16.20%
	Excited State 2	318.64	0.0647	HOMO→LUMO 87.64% HOMO→LUMO+1 9.11%
	Excited State 3	316.04	0.2353	HOMO−3→LUMO 2.40% HOMO−2→LUMO+1 6.94% HOMO−1→LUMO 14.78% HOMO→LUMO 9.63% HOMO→LUMO+1 61.78%
Method 2	Excited State 1	322.32	0.2286	HOMO−3→LUMO 4.41% HOMO−1→LUMO 74.55% HOMO→LUMO+1 16.20%
	Excited State 2	318.73	0.1006	HOMO−2→LUMO+1 2.15% HOMO→LUMO 80.24% HOMO→LUMO+1 15.17%
	Excited State 3	316.46	0.2182	HOMO−2→LUMO+1 5.73% HOMO−1→LUMO 14.63% HOMO→LUMO 17.13% HOMO→LUMO+1 56.36%
Method 3	Excited State 1	320.92	0.2286	HOMO−3→LUMO 2.05% HOMO−2→LUMO+1 2.35% HOMO−1→LUMO 56.50% HOMO→LUMO+1 36.56%
	Excited State 2	317.03	0.2870	HOMO−3→LUMO+1 5.59% HOMO−2→LUMO 5.27% HOMO−1→LUMO+1 24.63% HOMO→LUMO 61.60%

Table. S3 Photophysical data of metal ion probes. The amount of metal ion is 2 equivalents to the probe (1.0×10^{-5} mol dm^{-3} in MeCN).

	λ_{abs}/nm(ε/dm^3 mol^{-1}cm^{-1})	λ_{em}/nm	Φ
(*R*,*R*)-3-Cl	283(4.50×10^4); 322(1.74×10^3)	485	0.0049
(*R*,*R*)-3-Cl + Mg^{2+}	294(3.73×10^4);325(9.90×10^3); 385(1.01×10^4)	478	0.37
(*R*,*R*)-3-Cl + Zn^{2+}	294(3.73×10^4); 324(7.80×10^3); 384(1.05×10^4)	502	0.19
(*R*,*R*)-Naph	321(1.99×10^4); 355(1.45×10^4)	no emission	
(*R*,*R*)-Naph + Al^{3+}	321 (7.68×10^4); 402(6.06×10^4)	486.2	0.19
(*R*,*R*)-Naph + Zn^{2+}	326(1.46×10^4); 403(2.02×10^4)	528.6	0.021
(*R*,*R*)-Naph + Mg^{2+}	326(4.3×10^4); 403(3.29×10^4)	476.4	0.025

Table. S4 Photophysical data of anion probes. The amount of X^{-n} is 20 equivalents to the probe (1.0×10^{-5} mol dm^{-3} in DMSO).

	λ_{abs}/nm(ε/dm^3 mol^{-1}cm^{-1})	λ_{em}/nm	Φ
(*R*,*R*)-3-Cl	289(3.53×10^4); 323(1.31×10^4)	476	0.054
(*R*,*R*)-3-Cl + OH^-	291(1.59×10^4); 376(1.72×10^4)	470	0.23
(*R*,*R*)-3-Cl + F^-	294(3.41×10^4); 372(2.74×10^4)	467	0.23
(*R*,*R*)-3-Cl + CO_3^{2-}	288(3.93×10^4); 378(3.01×10^4)	474	0.23
(*R*,*R*)-3-Cl + AC^-	290(1.52×10^4); 377(1.68×10^4)	469	0.24
(*R*,*R*)-3-Cl + SO_3^{2-}	292(2.09×10^4); 381(1.29×10^4)	478	0.16
(*R*,*R*)-3-Cl + PO_4^{3-}	286(1.48×10^4); 379(1.65×10^4)	473	0.26
(*R*,*R*)-3-Cl + S^{2-}	378(3.29×10^4); 391(3.41×10^4)	464	0.003
(*R*,*R*)-3-Cl + $P_2O_7^{4-}$	292(1.71×10^4); 380(1.72×10^4)	470	0.25
(*R*,*R*)-3-Cl + HPO_4^{2-}	287(1.39×10^4); 375(1.64×10^4)	471	0.25
(*R*,*R*)-3-Cl + $H_2PO_4^-$	293(3.14×10^4); 318(1.45×10^4); 402(5.60×10^3)	481	0.013
(*R*,*R*)-3-Cl + Cl^-	297(3.44×10^4); 385(4.30×10^3)	480	0.044
(*R*,*R*)-3-Cl + Br^-	296(3.32×10^4); 388(4.80×10^3)	478	0.042
(*R*,*R*)-3-Cl + HCO_3^-	297(3.44×10^4); 385(4.31×10^3)	470	0.25
(*R*,*R*)-3-Cl + HS^-	291(1.67×10^4); 379(1.81×10^4)	472	0.23
(*R*,*R*)-3-Cl + I^-	287(3.19×10^4); 392(5.9×10^3)	477	0.030
(*R*,*R*)-3-Cl + SO_4^{2-}	291(3.57×10^4); 318(1.78×10^4);	477	0.007
(*R*,*R*)-3-Cl + HSO_3^-	294(3.58×10^4); 321(1.87×10^4);	481	0.004

Table. S5 Photophysical data of anion probes. The amount of X^{-n} is 20 equivalents to the probe (1.0×10^{-5} mol dm^{-3} in DMF).

	λ_{abs}/nm(ε/dm^3 mol^{-1}cm^{-1})	λ_{em}/nm	Φ
(*R*,*R*)-3-Cl	286(3.75×10^4); 323(1.74×10^4)	478	0.31
(*R*,*R*)-3-Cl + OH^-	283(2.20×10^4); 396(2.21×10^4)	483	0.21
(*R*,*R*)-3-Cl + F^-	285(2.08×10^4); 398(1.98×10^4)	490	0.40
(*R*,*R*)-3-Cl + CO_3^{2-}	286(2.52×10^4); 396(2.35×10^4)	488	0.20
(*R*,*R*)-3-Cl + AC^-	283(2.20×10^4); 396(2.21×10^4)	495	0.22
(*R*,*R*)-3-Cl + SO_3^{2-}	289(3.31×10^4); 396(8.40×10^3)	485	0.015
(*R*,*R*)-3-Cl + PO_4^{3-}	282(2.10×10^4); 393(1.97×10^4)	489	0.37
(*R*,*R*)-3-Cl + S^{2-}	270(4.08×10^4); 373(2.86×10^4)	475	0.17
(*R*,*R*)-3-Cl + $P_2O_7^{4-}$	289(2.33×10^4); 396(1.71×10^4)	489	0.15
(*R*,*R*)-3-Cl + HPO_4^{2-}	286(2.83×10^4); 400(1.86×10^4)	491	0.099
(*R*,*R*)-3-Cl + $H_2PO_4^-$	286(4.83×10^4); 322(2.73×10^4)	440	0.008
(*R*,*R*)-3-Cl + Cl^-	285(3.69×10^4); 382(7.20×10^3)	477	0.084
(*R*,*R*)-3-Cl + Br^-	293(3.73×10^4); 395(4.50×10^3)	478	0.039
(*R*,*R*)-3-Cl + HCO_3^-	287(2.43×10^4); 399(2.27×10^4)	495	0.21
(*R*,*R*)-3-Cl + HS^-	270(2.73×10^4); 383(1.91×10^4)	471	0.19
(*R*,*R*)-3-Cl + I^-	286(3.75×10^4); 387(6.00×10^3)	477	0.059
(*R*,*R*)-3-Cl + SO_4^{2-}	295(3.71×10^4); 385(6.01×10^3)	475	0.057
(*R*,*R*)-3-Cl + HSO_3^-	295(4.19×10^4); 321(1.92×10^4)	473	0.007

Table. S6 Photophysical data of anion probes. The amount of X^{-n} is 20 equivalents to the probe (1.0×10^{-5} mol dm^{-3} in EtOH).

	λ_{abs}/nm(ε/dm^3 mol^{-1}cm^{-1})	λ_{em}/nm	Φ
(*R*,*R*)-3-Cl	283(1.56×10^4); 323(1.51×10^4); 379(5.3×10^3)	481	0.045
(*R*,*R*)-3-Cl + OH^-	284(3.24×10^4); 369(2.70×10^4)	503	0.29
(*R*,*R*)-3-Cl +F^-	281(5.12×10^4); 320(2.02×10^4)	499	0.004
(*R*,*R*)-3-Cl + CO_3^{2-}	281(4.12×10^4); 363(8.80×10^4)	500	0.042
(*R*,*R*)-3-Cl + AC^-	283(4.62×10^4); 373(9.80×10^3)	481	0.13
(*R*,*R*)-3-Cl + SO_3^{2-}	282(3.09×10^4); 373(9.8×10^3)	484	0.004
(*R*,*R*)-3-Cl + PO_4^{3-}	281(4.98×10^4); 365(5.39×10^4)	504	0.32
(*R*,*R*)-3-Cl + S^{2-}	281(7.09×10^4); 364(5.12×10^4)	502	0.28
(*R*,*R*)-3-Cl + $P_2O_7^{4-}$	281(9.37×10^4); 367(6.15×10^4)	501	0.023
(*R*,*R*)-3-Cl + HPO_4^{2-}	281(8.09×10^4); 365(6.00×10^4)	504	0.085
(*R*,*R*)-3-Cl + $H_2PO_4^-$	281(7.24×10^4); 369(2.15×10^4)	502	0.005
(*R*,*R*)-3-Cl + Cl^-	284(4.39×10^4); 378(1.28×10^4)	477	0.18
(*R*,*R*)-3-Cl + Br^-	281(4.12×10^4); 373(8.97×10^3)	475	0.001
(*R*,*R*)-3-Cl + HCO_3^-	281(8.29×10^4); 365(7.15×10^4)	501	0.30
(*R*,*R*)-3-Cl + HS^-	281(4.02×10^4); 318(1.50×10^4)	485	0.042
(*R*,*R*)-3-Cl + I^-	282(4.48×10^4); 374(8.60×10^3)	479	0.14
(*R*,*R*)-3-Cl + SO_4^{2-}	282(6.79×10^4); 367(6.12×10^4)	499	0.005
(*R*,*R*)-3-Cl + HSO_3^-	279(7.57×10^4); 319(4.03×10^4);	479	0.010

Table. S7 Photophysical data of anion probes. The amount of X^{-n} is 20 equivalents to the probe (1.0×10^{-5} mol dm^{-3} in DMF).

	λ_{abs}/nm(ε/dm^3 mol^{-1}cm^{-1})	λ_{em}/nm	Φ
(*R*,*R*)-3,5-Cl	286(2.84×10^4); 333(1.04×10^4); 411(5.80×10^3)	490	0.012
(*R*,*R*)-3,5-Cl + OH^-	264(2.95×10^4); 387(1.41×10^4)	480	0.27
(*R*,*R*)-3,5-Cl + F^-	264(4.12×10^4); 387(1.49×10^4)	477	0.24
(*R*,*R*)-3,5-Cl + CO_3^{2-}	266(4.31×10^4); 392(1.62×10^4)	480	0.25
(*R*,*R*)-3,5-Cl + AC^-	386(1.43×10^4)	476	0.26
(*R*,*R*)-3,5-Cl + SO_3^{2-}	268(2.12×10^4); 396(1.24×10^4)	484	0.14
(*R*,*R*)-3,5-Cl + PO_4^{3-}	385(1.52×10^4)	478	0.24
(*R*,*R*)-3,5-Cl + S^{2-}	269(3.27×10^4); 394(1.73×10^4)	483	0.25
(*R*,*R*)-3,5-Cl + $P_2O_7^{4-}$	267(2.74×10^4); 392(1.51×10^4)	477	0.25
(*R*,*R*)-3,5-Cl + HPO_4^{2-}	269(2.67×10^4); 392(1.65×10^4)	473	0.23
(*R*,*R*)-3,5-Cl + $H_2PO_4^-$	333(1.69×10^4); 416(8.90×10^3)	484	0.007
(*R*,*R*)-3,5-Cl + Cl^-	288(2.50×10^4); 400(8.90×10^3);	485	0.071
(*R*,*R*)-3,5-Cl + Br^-	287(2.33×10^4); 395(9.10×10^3)	485	0.26
(*R*,*R*)-3,5-Cl + HCO_3^-	386(1.60×10^4)	478	0.24
(*R*,*R*)-3,5-Cl + HS^-	262(7.42×10^4);393(1.47×10^4)	480	0.24
(*R*,*R*)-3,5-Cl + I^-	333(6.70×10^3); 401(1.01×10^3)	484	0.086
(*R*,*R*)-3,5-Cl + SO_4^{2-}	289(2.44×10^4); 333(8.20×10^3); 401(8.20×10^3);	484	0.059
(*R*,*R*)-3,5-Cl + HSO_3^-	288(3.25×10^4); 344(1.53×10^4)	487	0.001

Table. S8 Photophysical data of the probe (1.0×10^{-5} mol dm^{-3} in DMSO) upon the addition of 100 equivalents of different amino acids.

	λ_{abs}/nm(ε/dm^3 mol^{-1}cm^{-1})	λ_{em}/nm	Φ
(*R*,*R*)-3,5-Cl	285(4.29×10^4); 331(1.70×10^4); 411(4.61×10^3)	441	0.004
(*R*,*R*)-3,5-Cl + *D*-Ala	301(8.50×10^3); 402(1.83×10^4)	490	0.21
(*R*,*R*)-3,5-Cl + *L*-Ala	300(1.16×10^4); 398(1.64×10^4)	487	0.20
(*R*,*R*)-3,5-Cl + *D*-Trp	335(1.64×10^4); 396(5.40×10^3)	476	0.24
(*R*,*R*)-3,5-Cl + *L*-Trp	338(1.25×10^4); 394(1.01×10^4)	480	0.11
(*R*,*R*)-3,5-Cl + *D*-Pro	300(1.23×10^4); 403(1.51×10^4)	486	0.17
(*R*,*R*)-3,5-Cl+ *L*-Pro	301(7.30×10^3); 394(1.61×10^4)	485	0.22
(*R*,*R*)-3,5-Cl + *D*-Glu	301(2.41×10^4); 333(1.73×10^4)	468	0.032
(*R*,*R*)-3,5-Cl + *L*-Glu	301(2.59×10^4); 333(1.79×10^4)	472	0.037
(*R*,*R*)-3,5-Cl + *D*-Val	301(1.43×10^4); 402(1.19×10^4)	483	0.13
(*R*,*R*)-3,5-Cl + *L*-Val	300(8.1×10^3); 398(1.91×10^4)	486	0.22
(*R*,*R*)-3,5-Cl + *D*-Arg	300(2.48×10^4); 393(2.72×10^4)	488	0.32
(*R*,*R*)-3,5-Cl + *L*-Arg	301(1.09×10^4); 390(2.08×10^4)	488	0.32
(*R*,*R*)-3,5-Cl + *D*-Leu	300(1.39×10^4); 396(6.5×10^3)	476	0.068
(*R*,*R*)-3,5-Cl + *L*-Leu	300(1.05×10^4); 403(1.65×10^4)	485	0.18
(*R*,*R*)-3,5-Cl + *D*-Ser	287(3.74×10^4); 339(1.57×10^4); 407(2.62×10^4)	491	0.21
(*R*,*R*)-3,5-Cl + *L*-Ser	262(1.46×10^4); 301(8.20×10^3); 394(1.17×10^4)	483	0.24
(*R*,*R*)-3,5-Cl + *D*-His	301(1.05×10^4); 399(1.47×10^4)	489	0.19
(*R*,*R*)-3,5-Cl + *L*-His	300(1.18×10^4); 403(1.82×10^4)	489	0.21
(*R*,*R*)-3-Cl	289(3.53×10^4); 323(1.31×10^4)	476	0.054
(*R*,*R*)-3-Cl + *D*-Ala	287(3.48×10^4); 296(3.38×10^4); 399(5.70×10^3)	489	0.025
(*R*,*R*)-3-Cl + *L*-Ala	259(3.31×10^4); 283(3.76×10^4); 394(4.10×10^3)	479	0.008
(*R*,*R*)-3-Cl + *D*-Trp	291(3.35×10^4); 394(5.60×10^3)	479	0.008
(*R*,*R*)-3-Cl+ *L*-Trp	287 (3.35×10^4); 394(5.15×10^3)	477	0.016
(*R*,*R*)-3-Cl + *D*-Pro	293(3.63×10^4); 400(3.70×10^3)	479	0.013
(*R*,*R*)-3-Cl + *L*-Pro	288(3.60×10^4); 394(4.50×10^3)	484	0.017
(*R*,*R*)-3-Cl + *D*-Glu	290(3.66×10^4); 224(1.78×10^4); 394(3.00×10^3)	480	0.021
(*R*,*R*)-3-Cl+ *L*-Glu	287(3.81×10^4); 293(3.82×10^4); 320(1.87×10^4)	480	0.005
(*R*,*R*)-3-Cl + *D*-Val	285(3.6×10^4); 298(3.67×10^4)	477	0.012

(*R*,*R*)-3-Cl + *L*-Val	294(3.27×10^4); 298(1.13×10^4)	484	0.073
(*R*,*R*)-3-Cl + *D*-Arg	289(2.47×10^4); 388(2.25×10^4)	484	0.26
(*R*,*R*)-3-Cl + *L*-Arg	286(3.86×10^4); 396(2.08×10^4)	487	0.15
(*R*,*R*)-3-Cl + *D*-Leu	290(3.15×10^4); 396(8.70×10^3)	482	0.052
(*R*,*R*)-3-Cl + *L*-Leu	289(3.35×10^4); 394(5.70×10^3)	481	0.036
(*R*,*R*)-3-Cl + *D*-Ser	296(3.52×10^4); 394(4.00×10^3)	479	0.024
(*R*,*R*)-3-Cl + *L*-Ser	297(3.56×10^4); 400(3.60×10^3)	480	0.008
(*R*,*R*)-3-Cl + *D*-His	290(3.63×10^4); 394(3.50×10^3)	483	0.015
(*R*,*R*)-3-Cl + *L*-His	289(3.83×10^4); 398(4.60×10^3)	479	0.018

Table. S9 Photophysical data of the probe (1.0×10^{-5} mol dm^{-3} in DMSO) upon the addition of 100 equivalents of different chiral substances.

	λ_{abs}/nm(ε/dm^3 mol^{-1}cm^{-1})	λ_{em}/nm	Φ	*ef*
(*R*,*R*)-3-Cl	289(3.53×10^4); 323(1.31×10^4)	476	0.054	
(*R*,*R*)-3-Cl + (*S*,*S*)DACH	284(3.13×10^4); 397(2.09×10^4)	476	0.17	0.75
(*R*,*R*)-3-Cl + (*R*,*R*)DACH	281(4.39×10^4); 399(3.43×10^4)	473	0.22	
(*R*,*R*)-3-Cl + (*S*)MEA	398(1.26×10^4)	475	0.06	0.87
(*R*,*R*)-3-Cl + (*R*)MEA	396(2.18×10^4)	476	0.07	
(*R*,*R*)-3-Cl + (*S*,*S*)DPEDA	283(4.46×10^4); 385(7.20×10^4)	476	0.07	1.09
(*R*,*R*)-3-Cl + (*R*,*R*)DPEDA	282(3.32×10^4); 387(2.19×10^4)	474	0.07	
(*R*,*R*)-3-Cl + (*S*)MM	287(2.87×10^4); 390(4.59×10^3)	478	0.13	0.38
(*R*,*R*)-3-Cl + (*R*)MM	288(2.89×10^4); 389(4.89×10^3)	476	0.28	
(*S*,*S*)-3-Cl	289(3.53×10^4); 323(1.31×10^4)	476	0.054	
(*S*,*S*)-3-Cl + (*S*,*S*)DACH	286(3.33×10^4); 399(2.19×10^4)	491	0.16	1.07
(*S*,*S*)-3-Cl + (*R*,*R*)DACH	285(3.39×10^4); 399(2.23×10^4)	491	0.16	
(*S*,*S*)-3-Cl + (*S*)MEA	401(1.45×10^4)	489	0.067	0.52
(*S*,*S*)-3-Cl + (*R*)MEA	397(1.74×10^4)	486	0.091	
(*S*,*S*)-3-Cl + (*S*,*S*)DPEDA	284(5.36×10^4); 387(8.3×10^4)	481	0.074	0.59
(*S*,*S*)-3-Cl + (*R*,*R*)DPEDA	285(4.30×10^4); 390(1.44×10^4)	481	0.096	
(*S*,*S*)-3-Cl + (*S*)MM	286(3.97×10^4); 389(5.91×10^3)	478	0.040	0.94
(*S*,*S*)-3-Cl + (*R*)MM	286(4.20×10^4); 389(4.90×10^3)	478	0.047	
(*R*,*R*)-3,5-Cl	285(4.29×10^4); 331(1.70×103); 411(4.60×10^4)	441	0.004	
(*R*,*R*)-3,5-Cl + (*S*,*S*)DACH	301(2.66×10^4); 333(1.85×10^4)	478	0.26	0.93
(*R*,*R*)-3,5-Cl + (*R*,*R*)DACH	300(2.67×10^4); 333(1.89×10^4)	478	0.29	
(*R*,*R*)-3,5-Cl + (*S*)MEA	388(2.10×10^4)	478	0.23	0.90
(*R*,*R*)-3,5-Cl + (*R*)MEA	393(2.24×10^4)	478	0.21	
(*R*,*R*)-3,5-Cl + (*S*,*S*)DPEDA	302(2.64×10^4); 395(1.44×10^4)	481	0.23	0.58
(*R*,*R*)-3,5-Cl + (*R*,*R*)DPEDA	300(2.69×10^4); 396(1.43×10^4)	484	0.15	
(*R*,*R*)-3,5-Cl + (*S*)MM	261(3.62×10^4); 300(2.63×10^4); 333(1.85×10^4)	482	0.025	1.02

(*R*,*R*)-3,5-Cl + (*R*)MM	265(2.08×10^4); 300(2.61×10^4); 333(1.81×10^4)	456	0.027	
(*S*,*S*)-3,5-Cl	285(4.29×10^4); 331(1.7×10^4); 411(4.6×10^3)	441	0.004	
(*S*,*S*)-3,5-Cl + (*S*,*S*)DACH	266(3.86×10^4); 390(1.92×10^4)	481	0.28	0.94
(*S*,*S*)-3,5-Cl + (*R*,*R*)DACH	263(5.17×10^4); 392(2.00×10^4)	479	0.26	
(*S*,*S*)-3,5-Cl + (*S*)MEA	395(1.83×10^4)	482	0.25	0.95
(*S*,*S*)-3,5-Cl + (*R*)MEA	394(2.12×10^4)	481	0.27	
(*S*,*S*)-3,5-Cl + (*S*,*S*) DPEDA	286(4.56×10^4); 396(1.49×10^4)	484	0.14	0.63
(*S*,*S*)-3,5-Cl + (*R*,*R*) DPEDA	286(4.68×10^4); 396(1.76×10^4)	482	0.22	
(*S*,*S*)-3,5-Cl + (*S*)MM	300(2.73×10^4); 333(1.53×10^4); 403(7.30×10^3)	478	0.066	3.95
(*S*,*S*)-3,5-Cl + (*R*)MM	287(4.25×10^4); 333(2.04×10^4)	448	0.010	

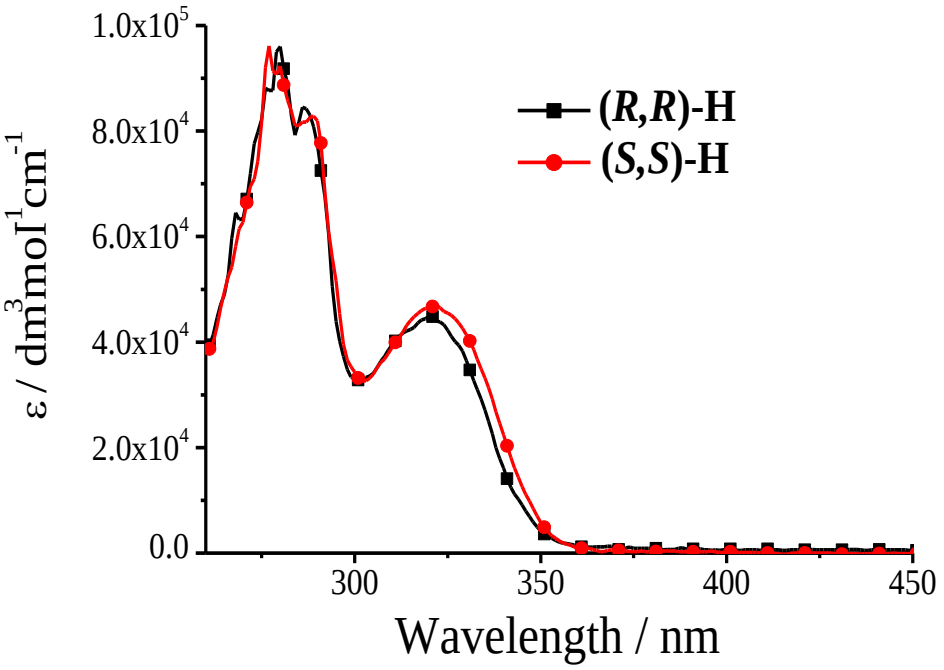

Fig. S1 Absorption spectra of (***R,R***)**-H** and (***S,S***)**-H** in MeCN (1.0×10^{-5} mol dm^{-3}).

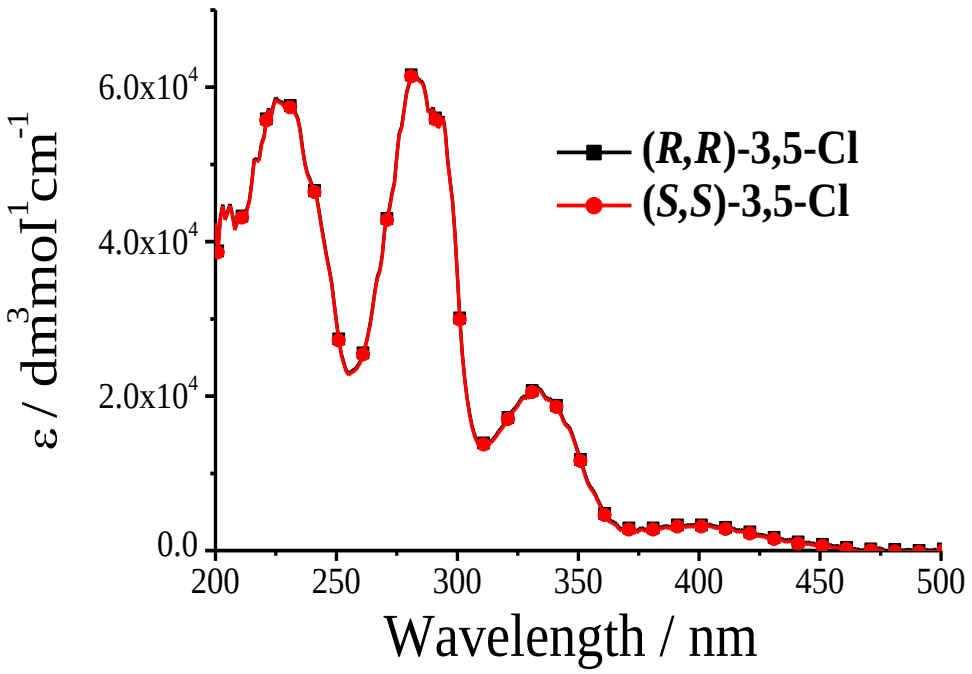

Fig. S2 Absorption spectra of (***R,R***)**-3,5-Cl** and (***S,S***)**-3,5-Cl** in MeCN (1.0×10^{-5} mol dm^{-3}).

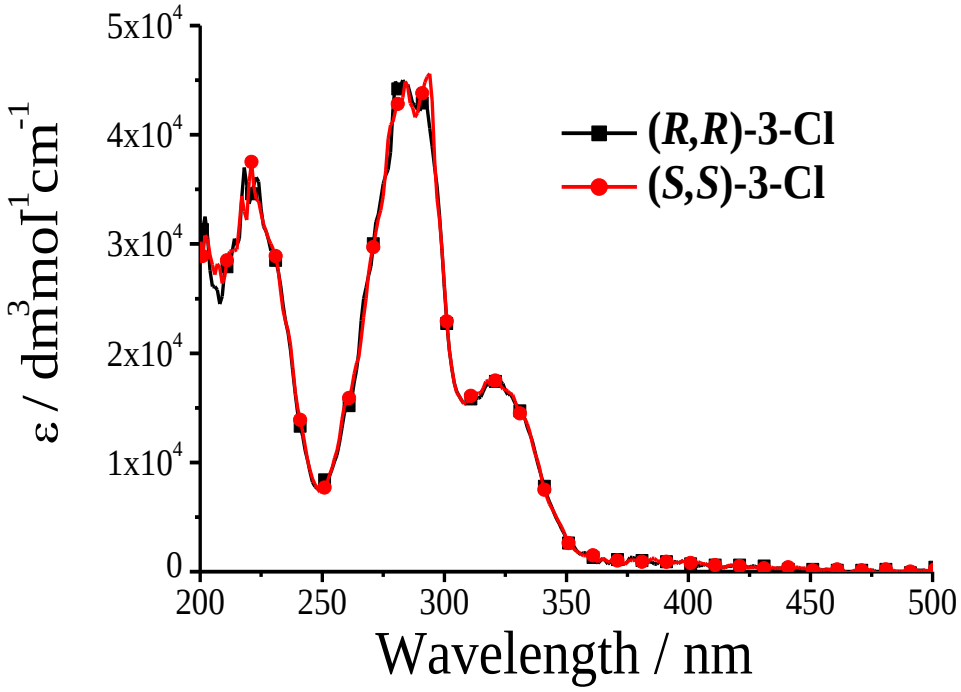

Fig. S3 Absorption spectra of (***R,R***)**-3-Cl** and (***S,S***)**-3-Cl** in MeCN (1.0×10^{-5} mol dm^{-3}).

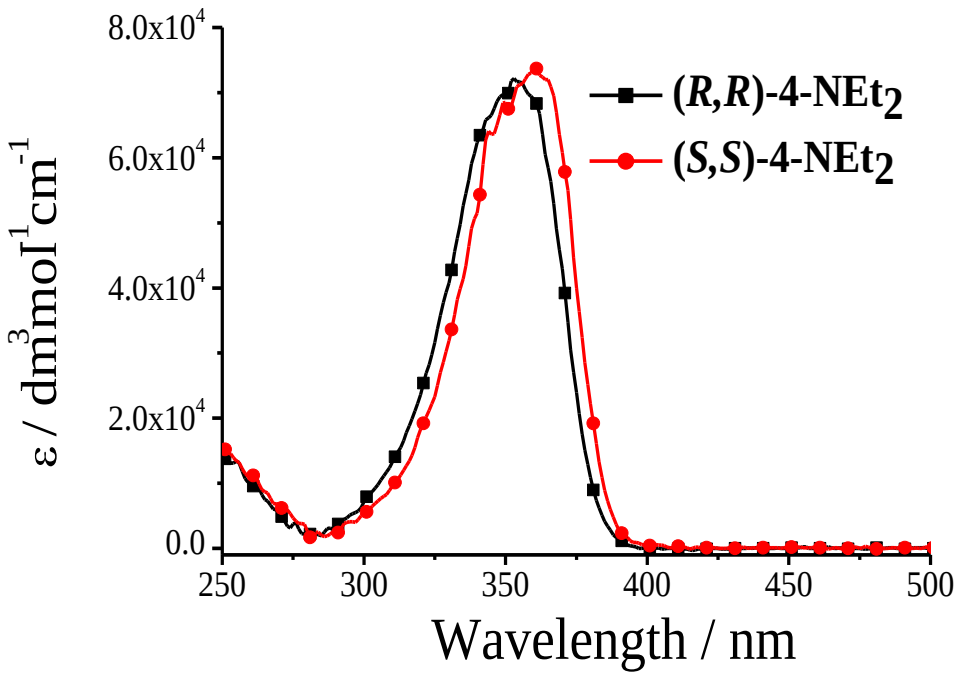

Fig. S4 Absorption spectra of (***R,R***)**-4-NEt$_2$** and (***S,S***)**-4-NEt$_2$** in MeCN (1.0×10^{-5} mol dm^{-3}).

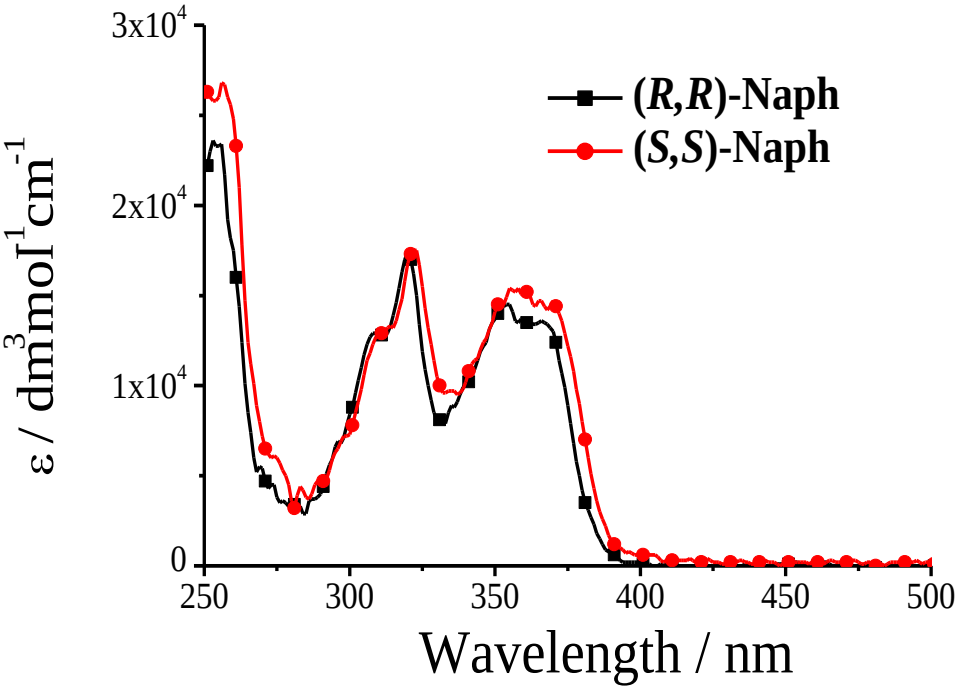

Fig. S5 Absorption spectra of **(*R*,*R*)-NaPh** and (***S*,*S*)-NaPh** in MeCN (1.0×10^{-5} mol dm^{-3}).

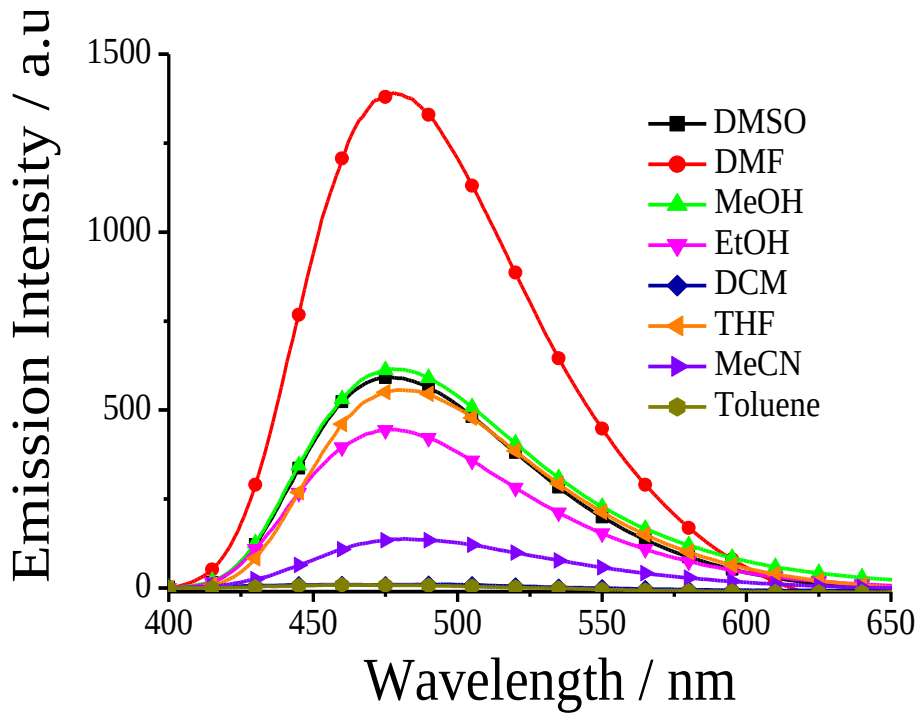

Fig. S6 Emission spectra of **(*R*,*R*)-H** in different solvents (1.0×10^{-5} mol dm^{-3}, excited at 380 nm).

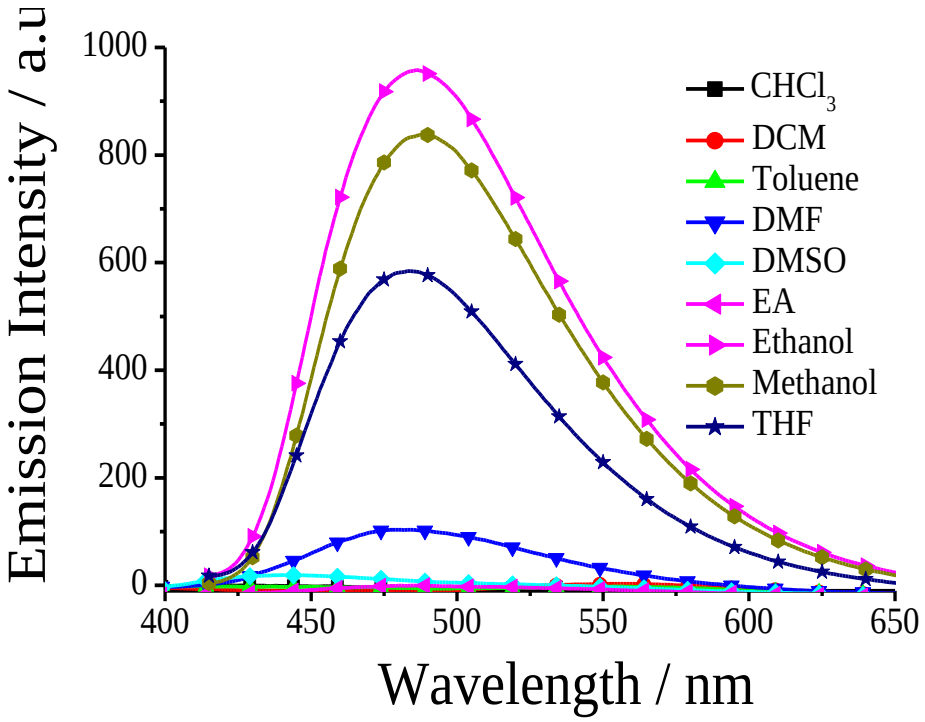

Fig. S7 Emission spectra of **(*R*,*R*)-3,5-Cl** in different solvents (1.0×10^{-5} mol dm^{-3}, excited at 390 nm).

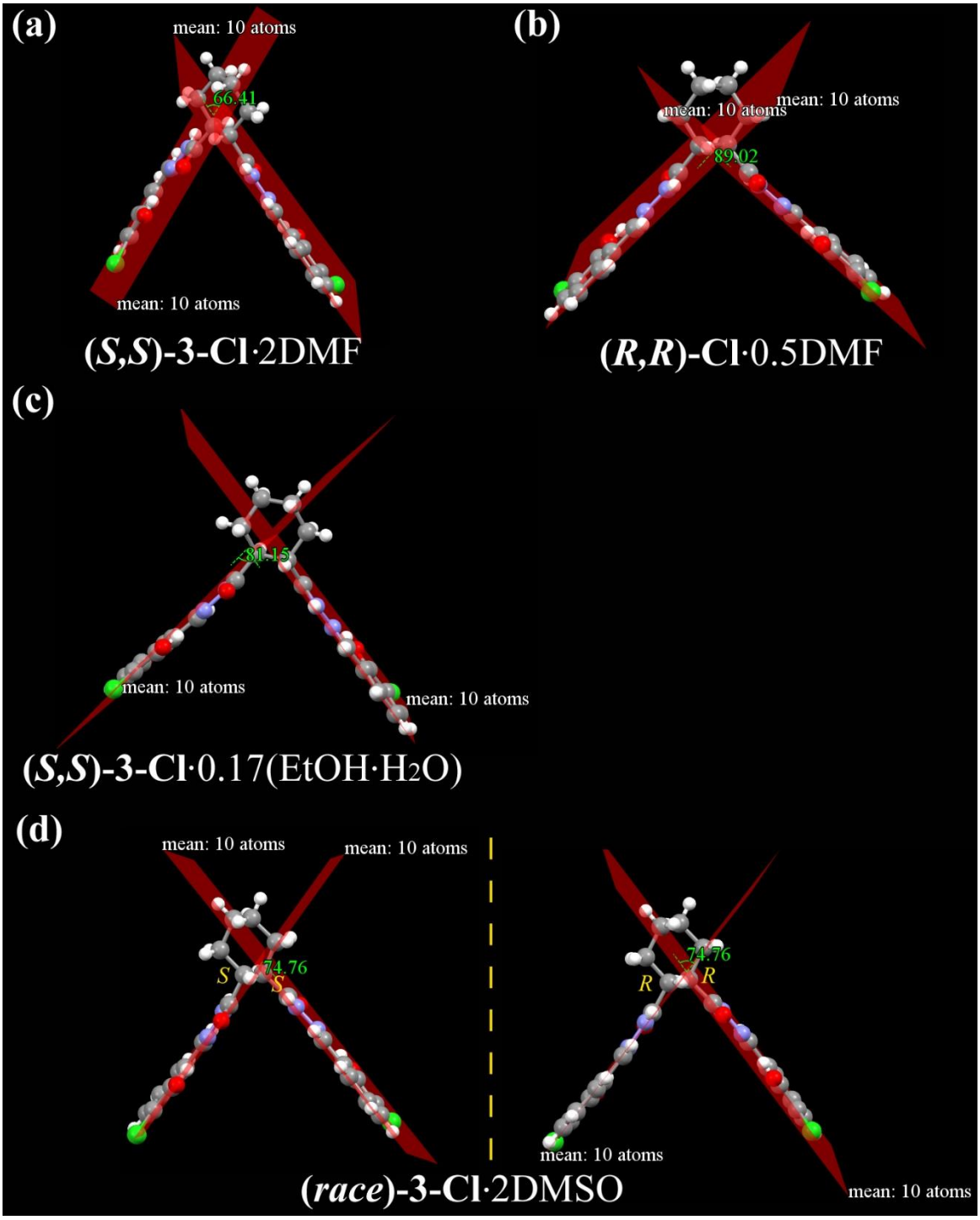

Fig. S8 Dihedral angles between two π-conjugation panels of **(*S*,*S*)-3−Cl**, **(*R*,*R*)-3-Cl**, and ***race*-3−Cl** molecules.

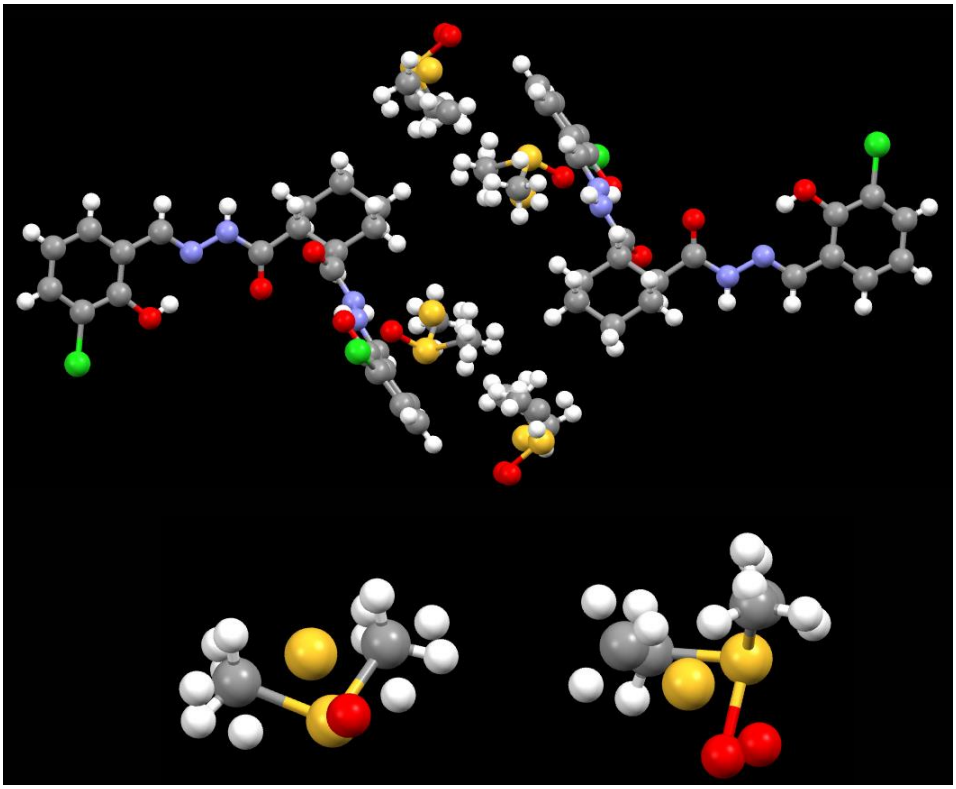

Fig. S9 Disorder problem of solvent in ***race*-3-Cl**·2DMSO single crystal.

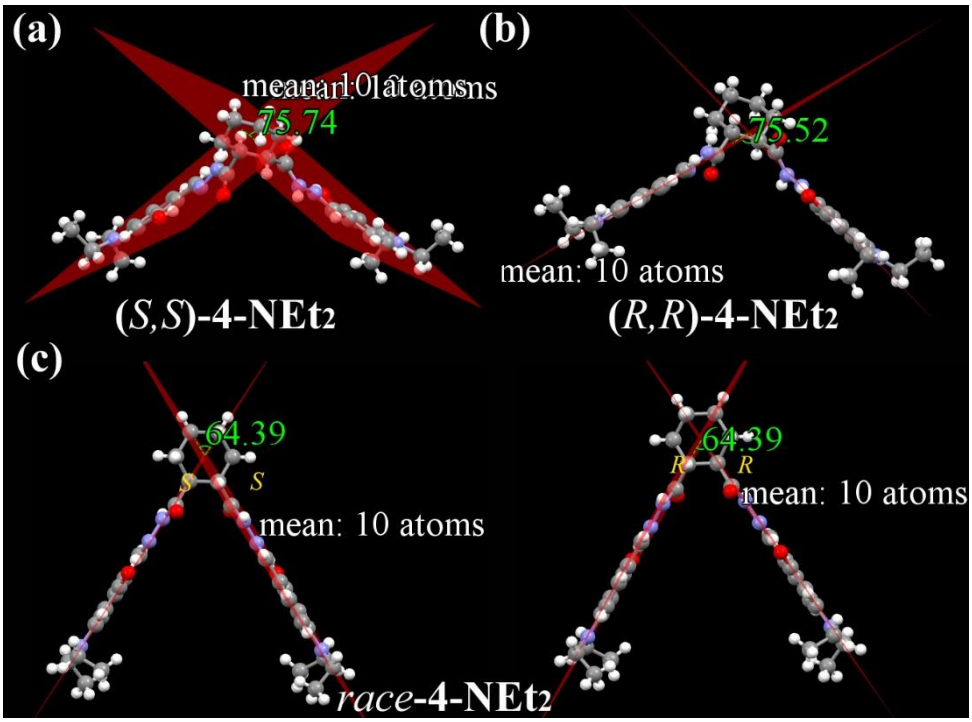

Fig. S10 Dihedral angles between two π-conjugation panels of**(*S*,*S*)-4-NEt2**, **(*R*,*R*)-4-NEt2**, and ***race*-4-NEt2**·$2H_2O$ molecules.

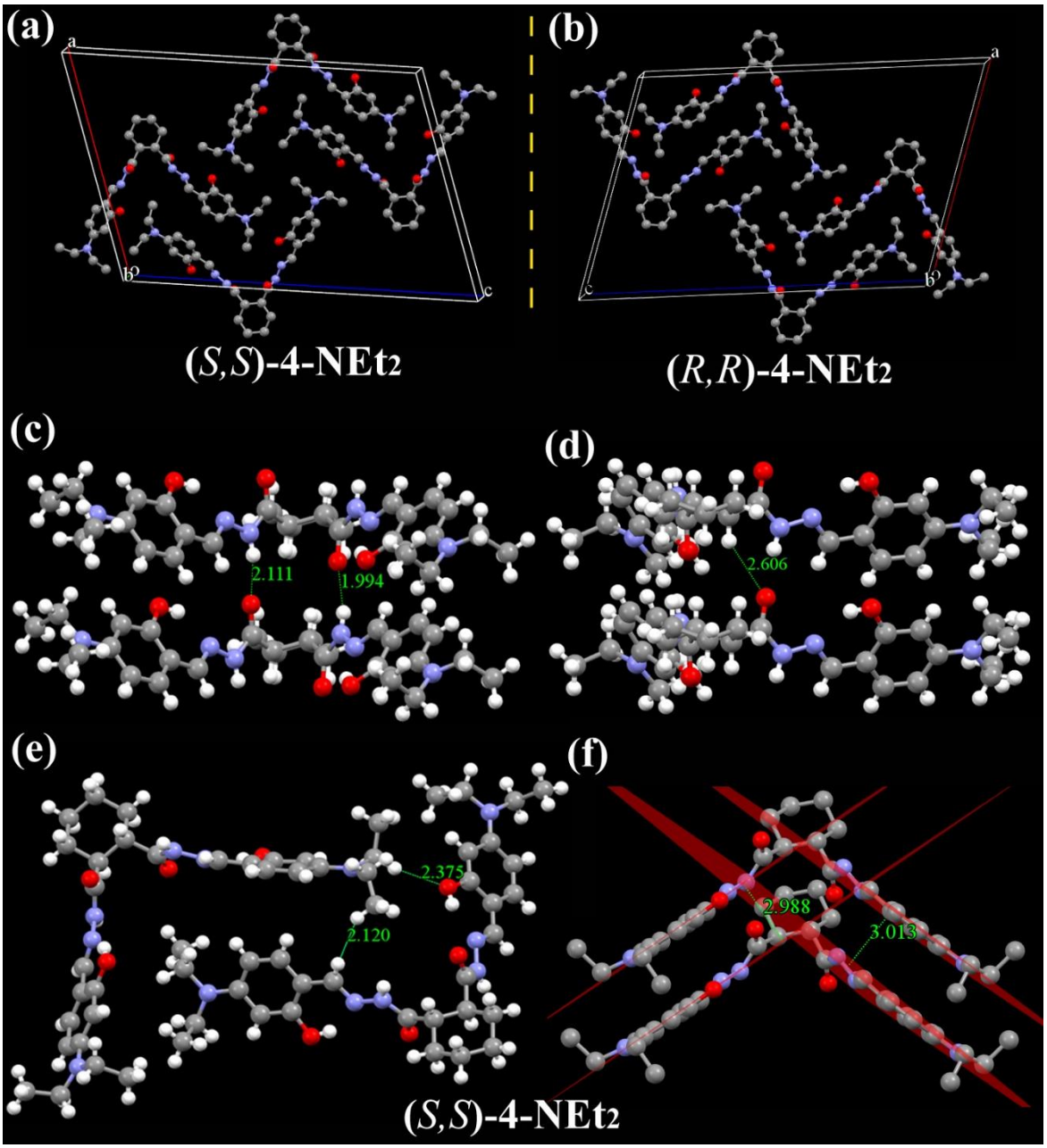

Fig. S11 X-ray single crystal structures and packing of **(*R*,*R*)-4-NEt$_2$** and **(*S*,*S*)-4-NEt$_2$** molecules: (a and b) packing in a unit cell (H atoms are omitted); (c) intermolecular interactions of the two closest **(*S*,*S*)-4-NEt$_2$** molecules; (d) the strongest intermolecular interaction between the non-conjugated cyclohexane bridges of the two adjacent **(*S*,*S*)-4-NEt$_2$** molecules; (e) intermolecular interactions of the two adjacent **(*S*,*S*)-4-NEt$_2$** molecules; (f) intermolecular π–π interactions between π-conjugations (salicylaldehyde hydrazide units) of the two closest **(*S*,*S*)-4-NEt$_2$** molecules (H atoms are omitted).

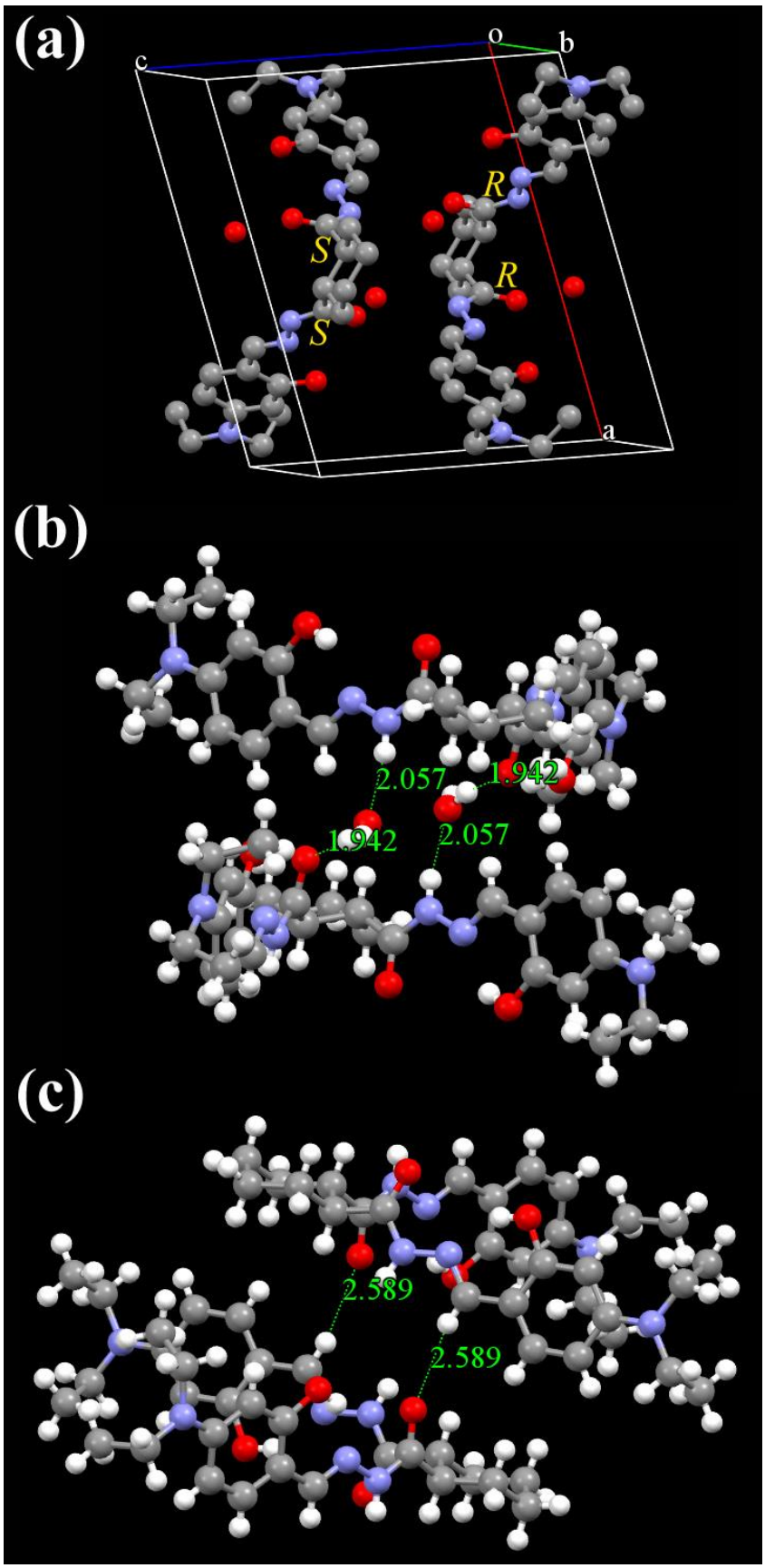

Fig. S12 X-ray single crystal structures and packing of ***race*-4-NEt$_2$·2H$_2$O** molecules: (a) packing in a unit cell (H atoms are omitted); (b and c) intermolecular interactions of the two closest molecules.

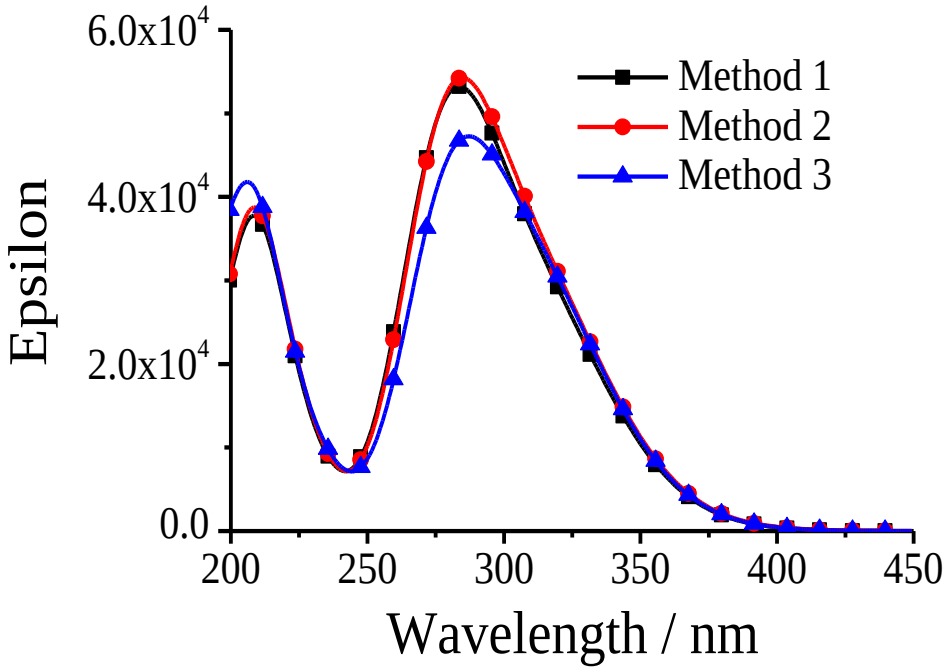

Fig. S13 Computational absorption spectra of **(*S*,*S*)-3-Cl**.

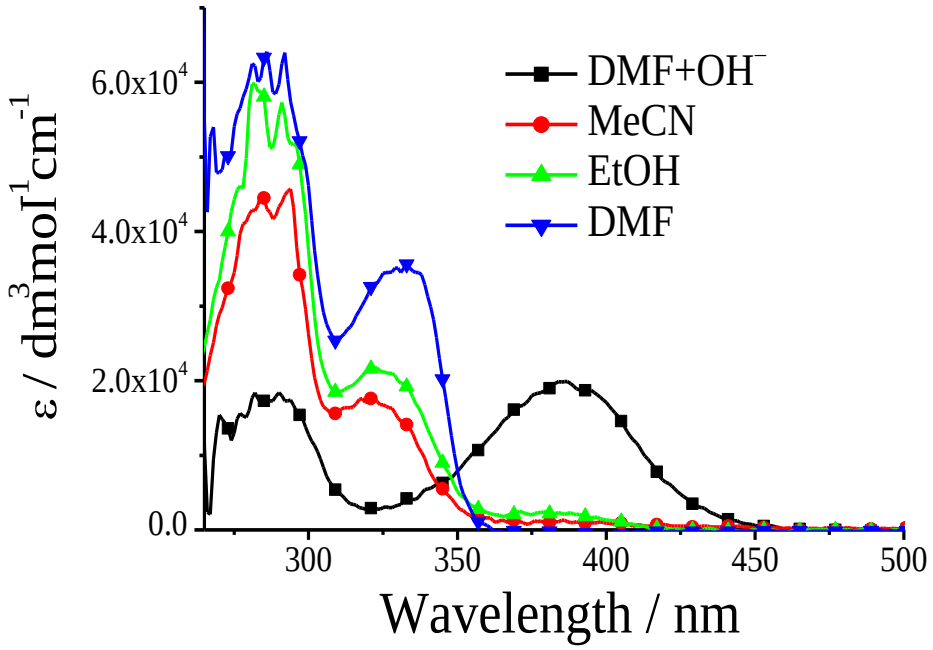

Fig. S14 Absorption spectra of **(*S*,*S*)-3-Cl** in different solvents [1.0×10^{-5} mol dm^{-3}, OH^- is is 20 equivalents to **(*S*,*S*)-3-Cl**].

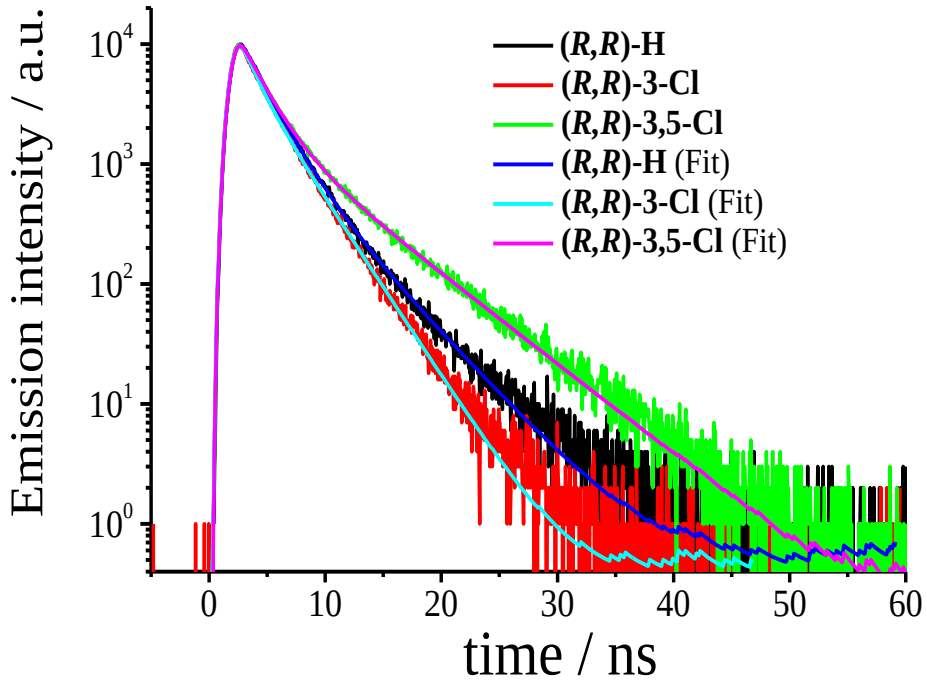

Fig. S15 Time-resolved emission decay spectra (excited at 370 nm, 1.0×10^{-5} mol dm^{-3} in DMF).

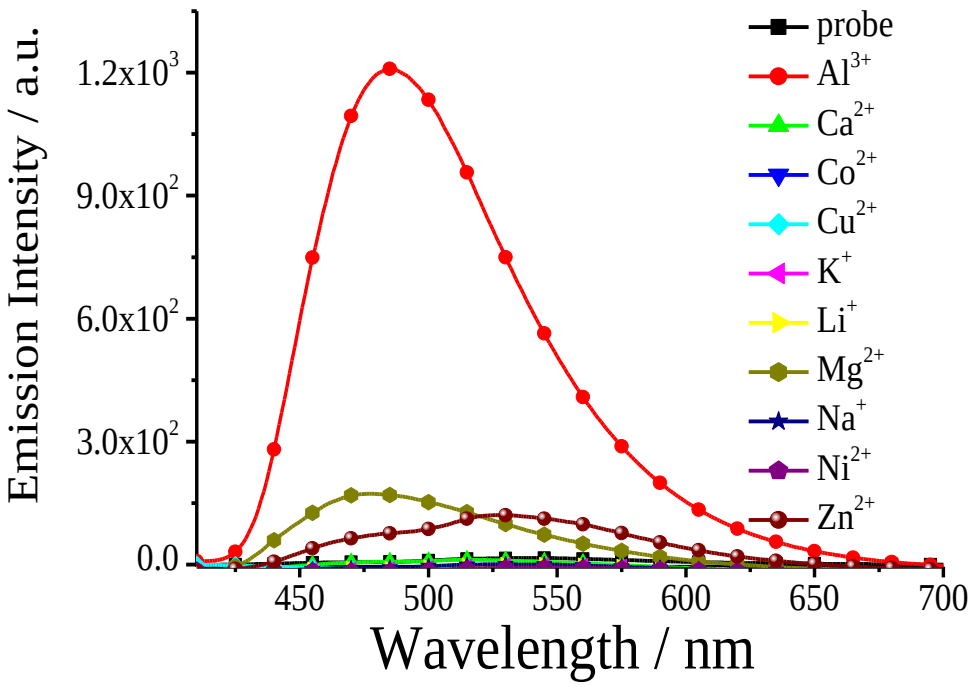

Figure. S16 Emission spectra of ***(R,R)*-NaPh** (1.0×10^{-5} mol dm^{-3} in EtOH, excited at 370 nm) upon the addition of 2 equivalents of different metal ions.

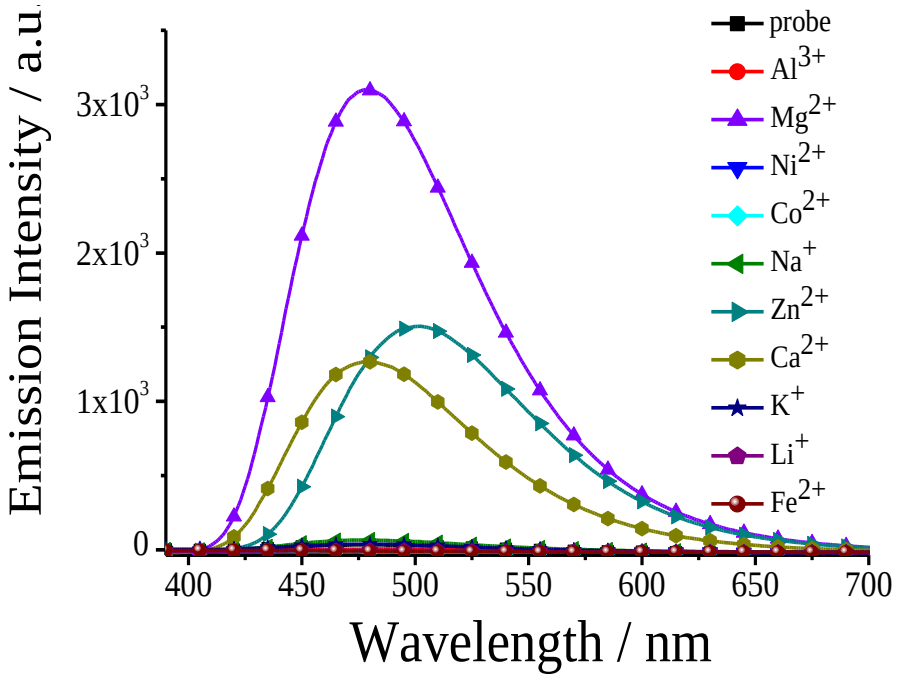

Figure. S17 Emission spectra of **(*R*,*R*)-3-Cl** (1.0×10^{-5} mol dm^{-3} in MeCN, excited at 370 nm) upon the addition of 2 equivalents of different metal ions.

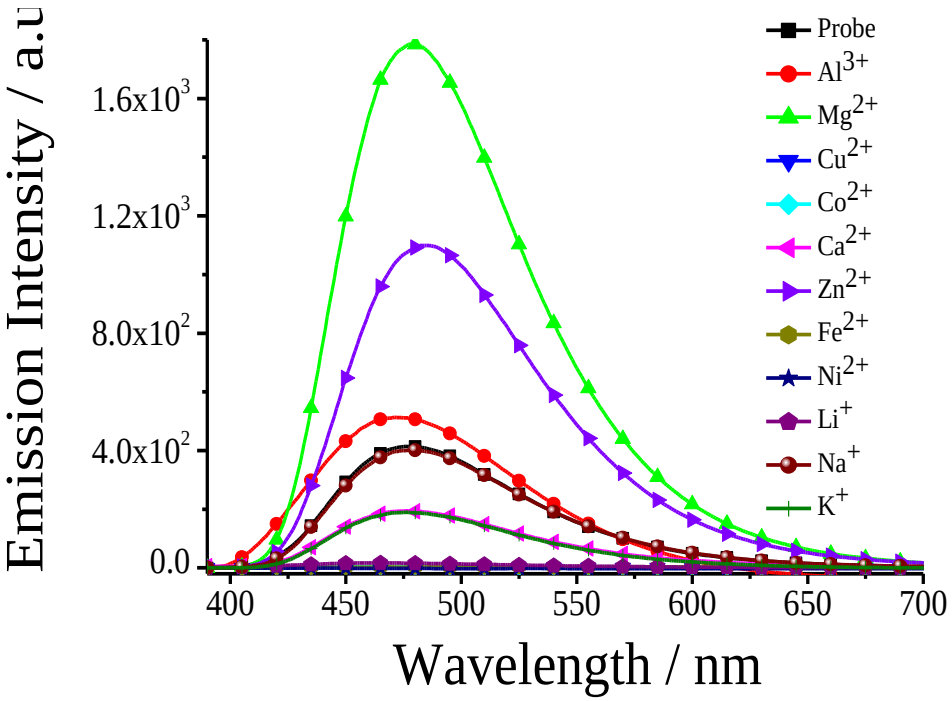

Figure. S18 Emission spectra of **(*R*,*R*)-3-Cl** (1.0×10^{-5} mol dm^{-3} in EtOH, excited at 370 nm) upon the addition of 2 equivalents of different metal ions.

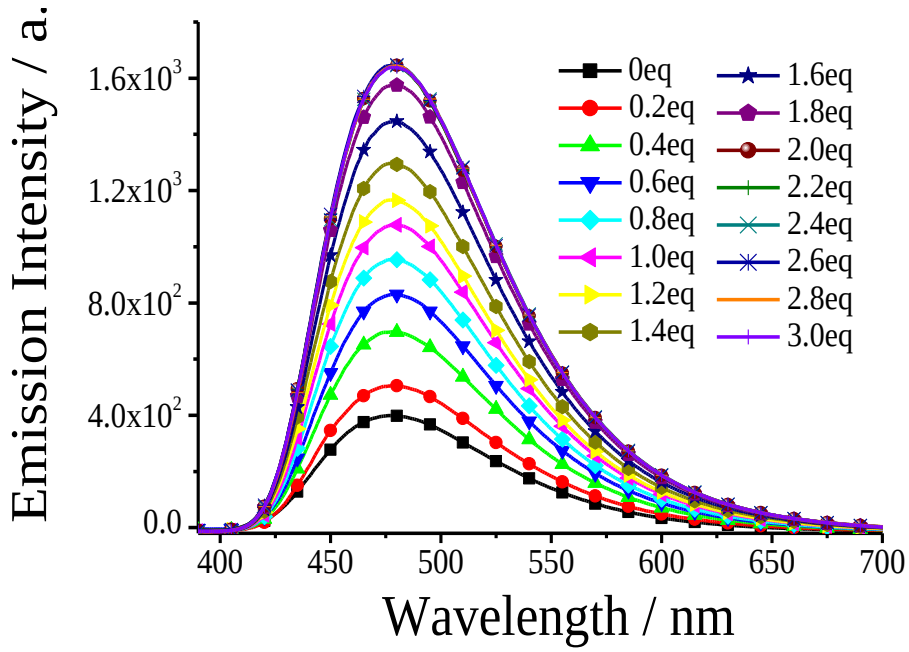

Figure. S19 Emission spectra of **(*R*,*R*)-3-Cl** (1.0×10^{-5} mol dm^{-3} in EtOH, excited at 370 nm) upon the addition of different equivalents of Mg^{2+}.

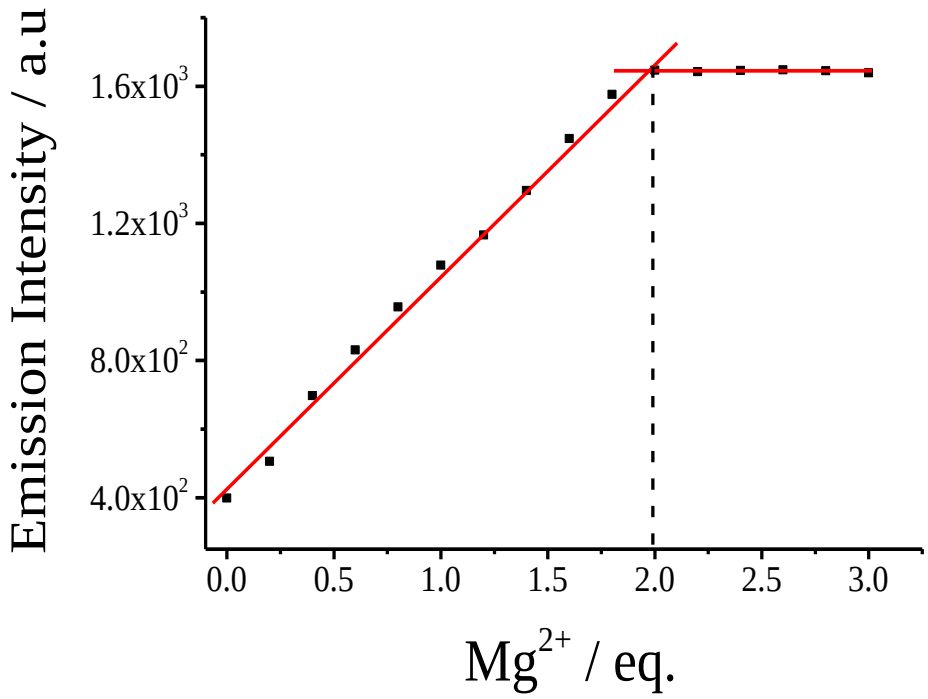

Figure. S20 Plot of emission intensity of **(*R*,*R*)-3-Cl** at 478 nm (1.0×10^{-5} mol dm^{-3} in EtOH, excited at 370 nm) as a function of different equivalents of Mg^{2+}.

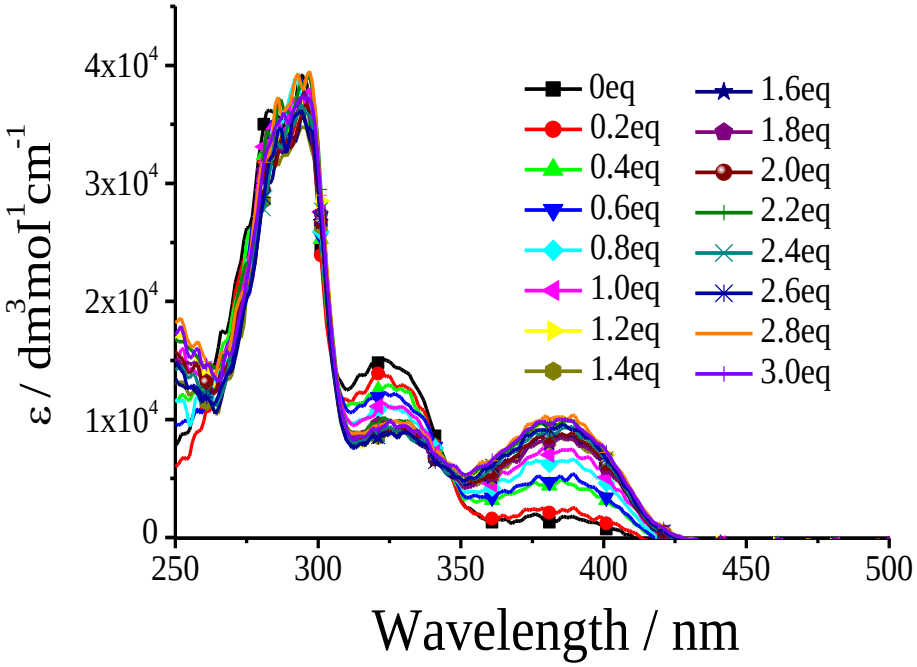

Figure. S21 Absorption spectra of **(*R*,*R*)-3-Cl** (1.0×10^{-5} mol dm^{-3} in EtOH) upon the addition of different equivalents of Mg^{2+}.

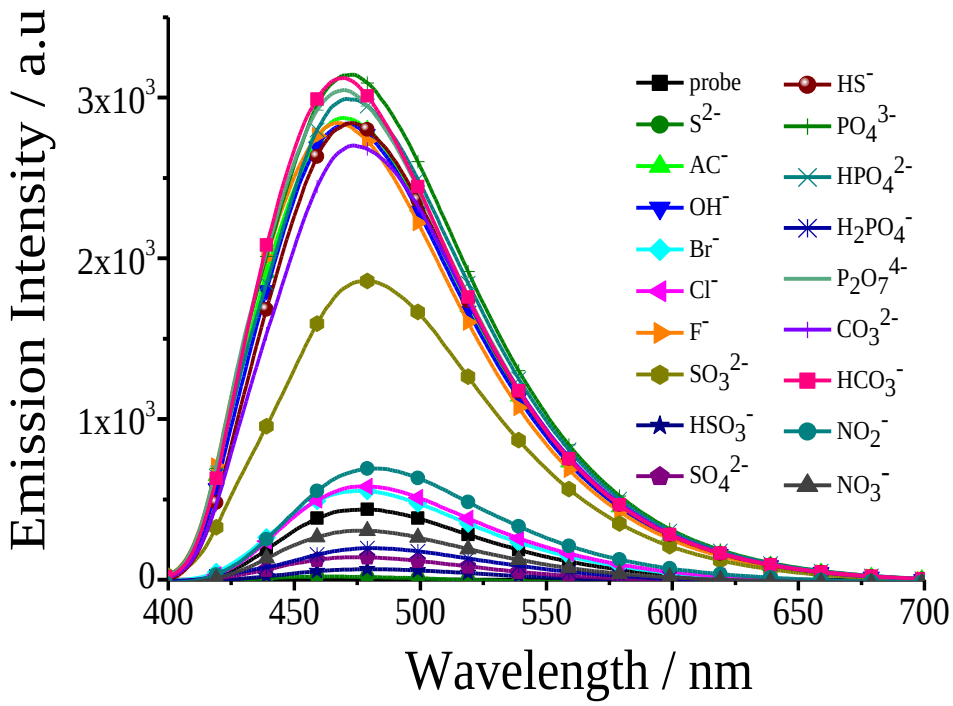

Figure. S22 Emission spectra of **(*R*,*R*)-3-Cl** (1.0×10^{-5} mol dm^{-3} in DMSO, excited at 370 nm) upon the addition of 20 equivalents of different anions.

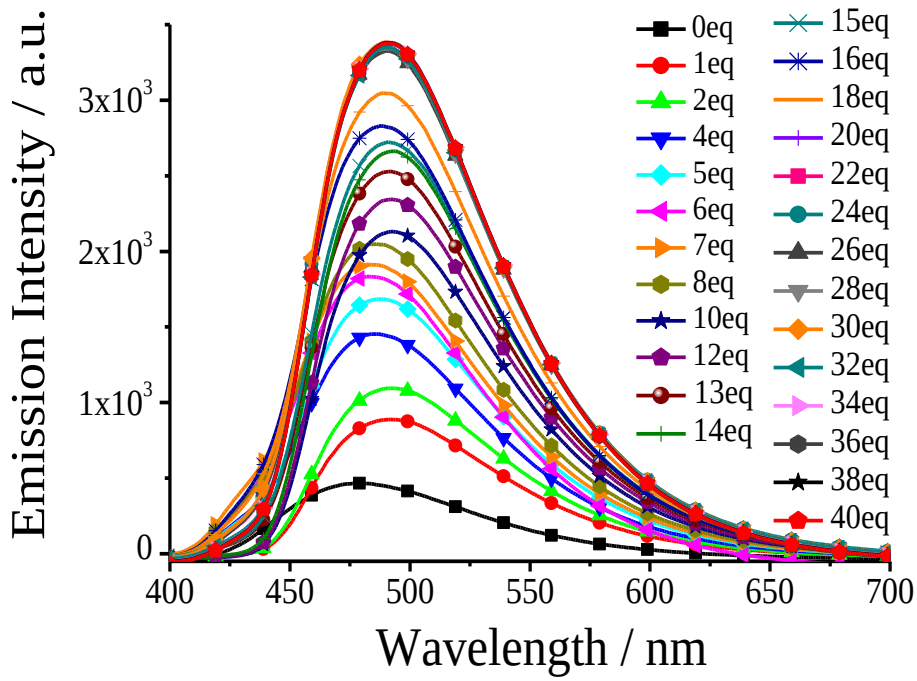

Fig. S23 Emission spectra of **(*R*,*R*)-3-Cl** (1.0×10^{-5} mol dm^{-3} in DMSO, excited at 370 nm) upon the addition of different equivalents of OH^-.

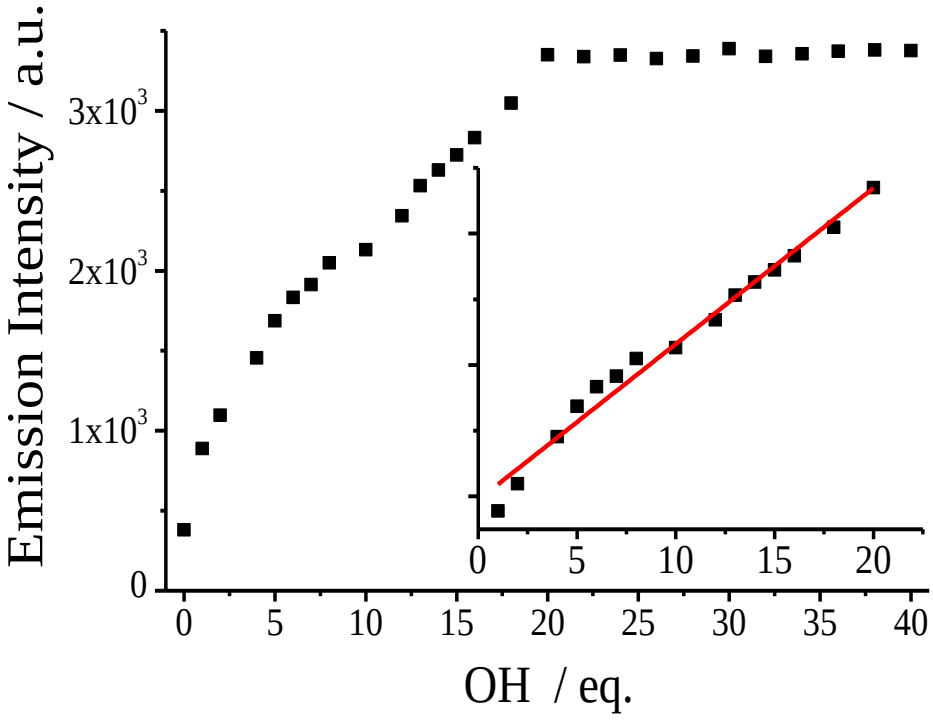

Fig. S24 Plot of emission intensity at 500 nm of **(*R*,*R*)-3-Cl** (1.0×10^{-5} mol dm^{-3} in DMSO, excited at 370 nm) as a function of OH^- concentration.

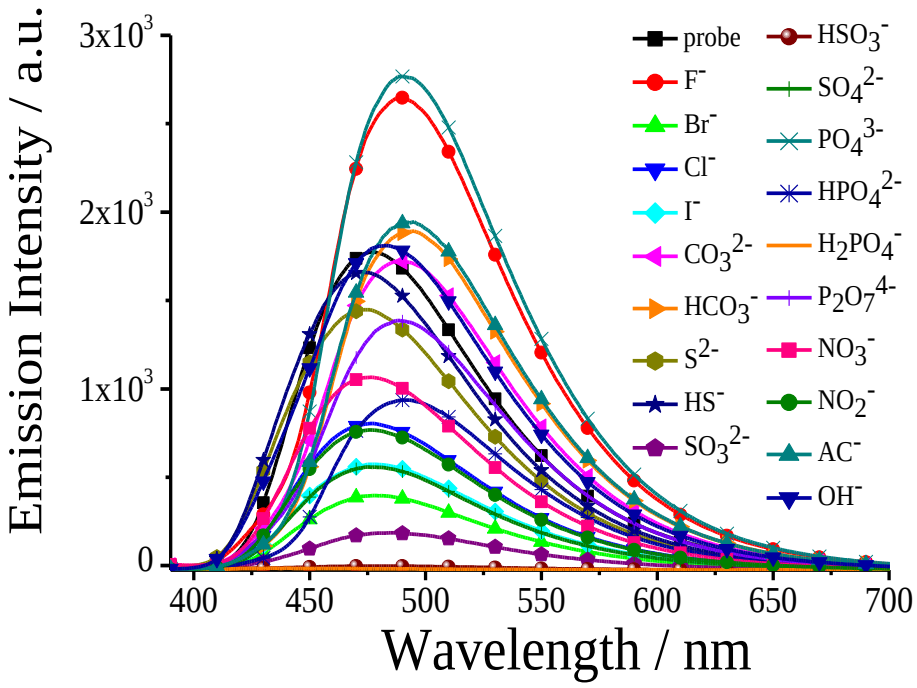

Figure. S25 Emission spectra of **(*R*,*R*)-3-Cl** (1.0×10^{-5} mol dm^{-3} in DMF, excited at 370 nm) upon the addition of 20 equivalents of different anions.

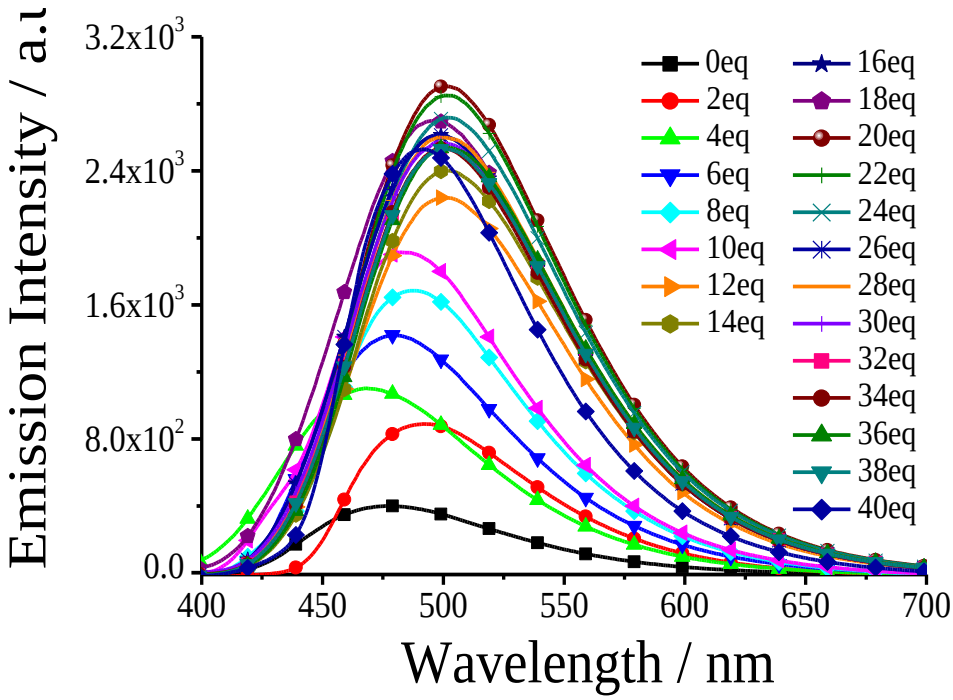

Fig. S26 Emission spectra of **(*R*,*R*)-3-Cl** (1.0×10^{-5} mol dm^{-3} in EtOH, excited at 370 nm) upon the addition of different equivalents of OH^-.

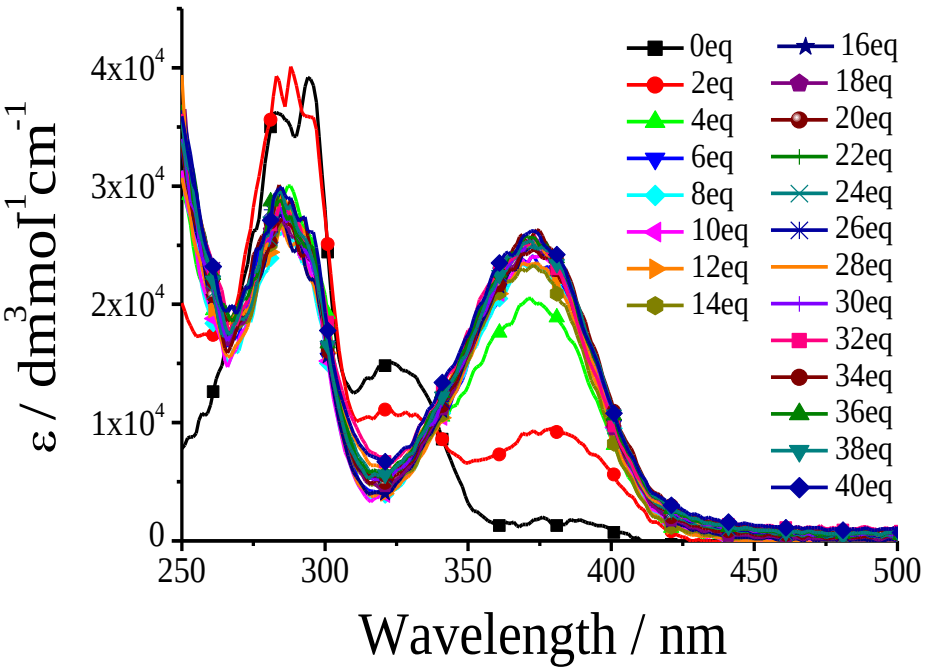

Fig. S27 Absorption spectra of **(*R*,*R*)-3-Cl** (1.0×10^{-5} mol dm^{-3} in EtOH) upon the addition of different equivalents of OH^-.

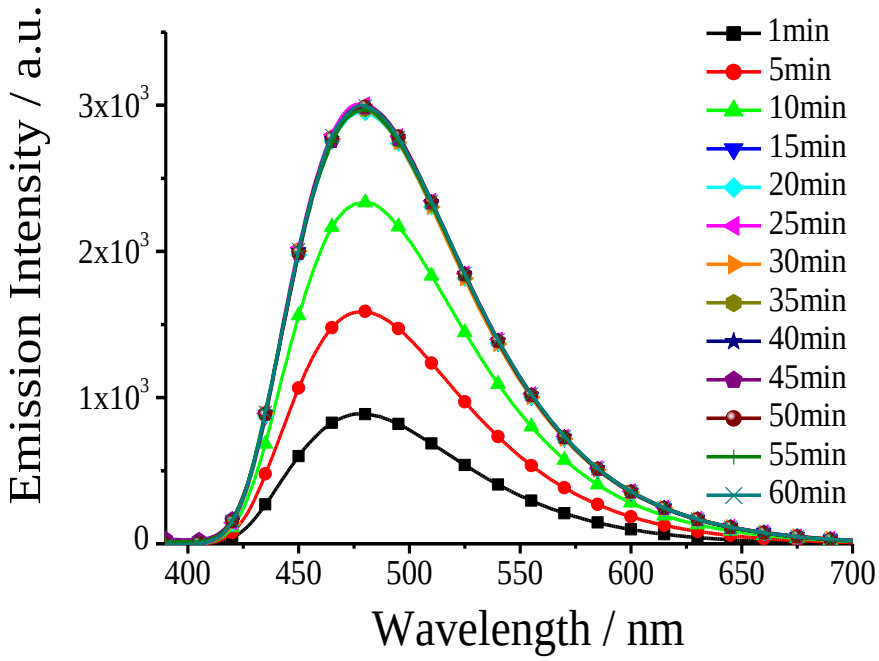

Fig. S28 Raction dynamics of emission spectra for **(*R*,*R*)-3-Cl** (1.0×10^{-5} mol dm^{-3} in EtOH, excited at 370 nm) after adding 2 equivalents Mg^{2+}.

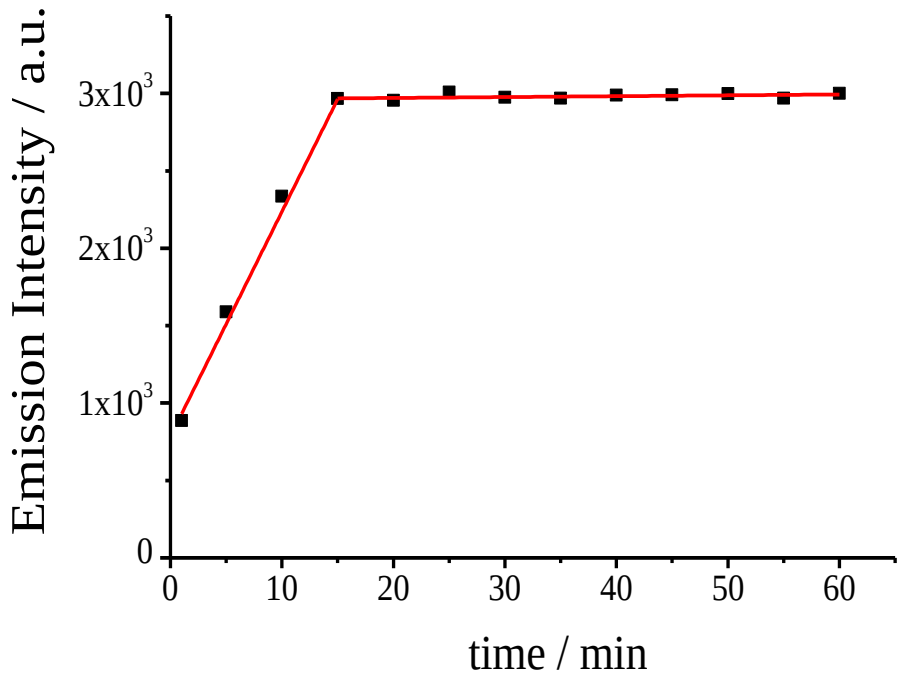

Fig. S29 Raction dynamics of emission intensity for **(*R*,*R*)-3-Cl** (1.0×10^{-5} mol dm^{-3} in ethanol, excited at 370 nm) at 470 nm after adding 2 equivalents of Mg^{2+}.

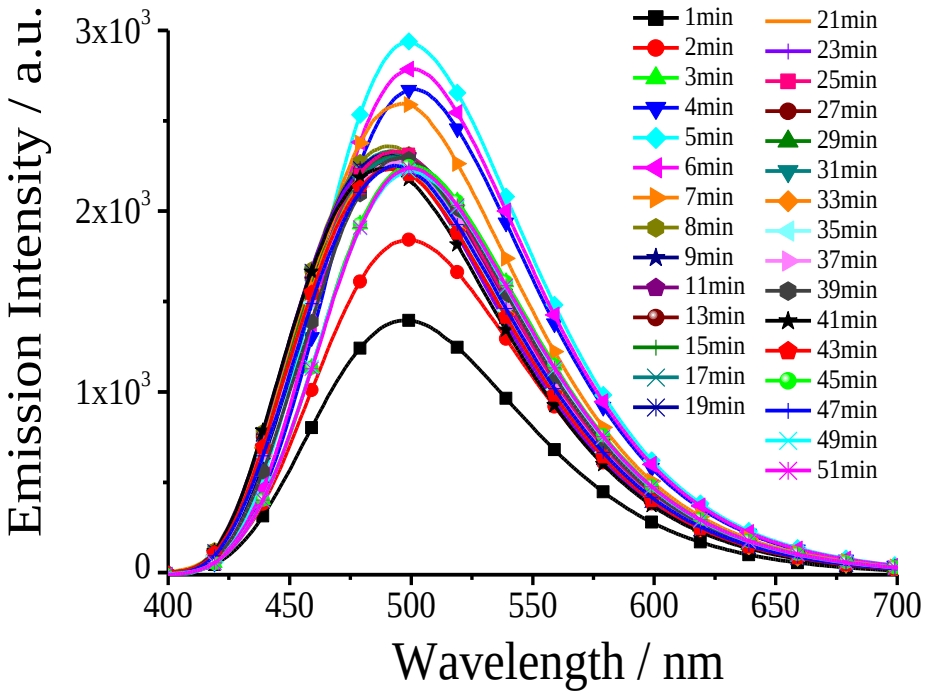

Fig. S30 Raction dynamics of emission spectra for **(*R*,*R*)-3-Cl** (1.0×10^{-5} mol dm^{-3} in EtOH, excited at 370 nm) after adding 20 equivalents OH^-.

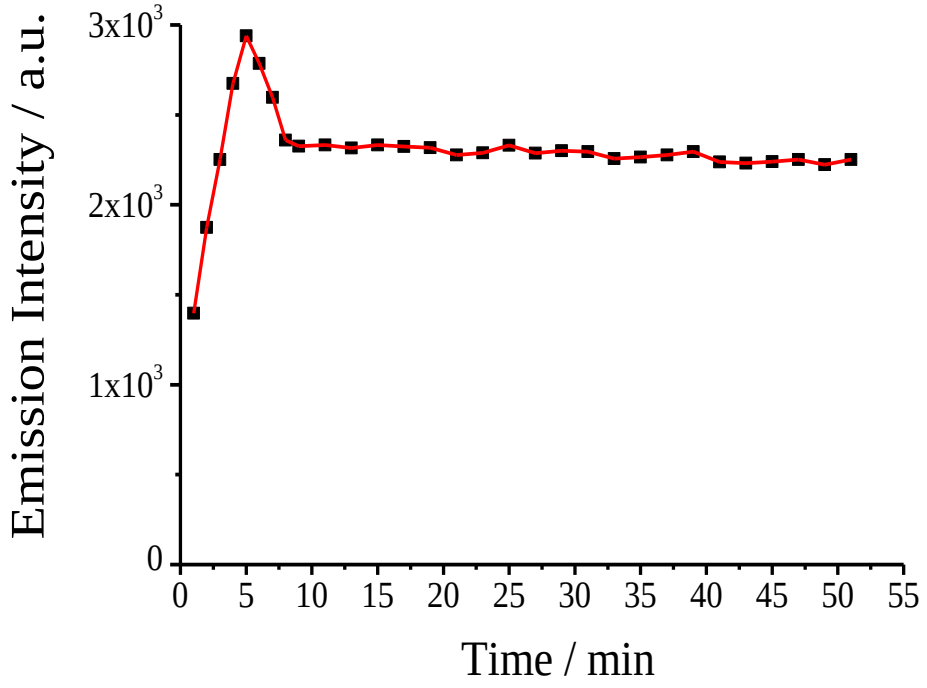

Fig. S31 Raction dynamics of emission intensity for **(*R*,*R*)-3-Cl** (1.0 × 10^{-5} mol dm^{-3} in ethanol, excited at 370 nm) at 503 nm after adding 20 equivalents of OH^-.

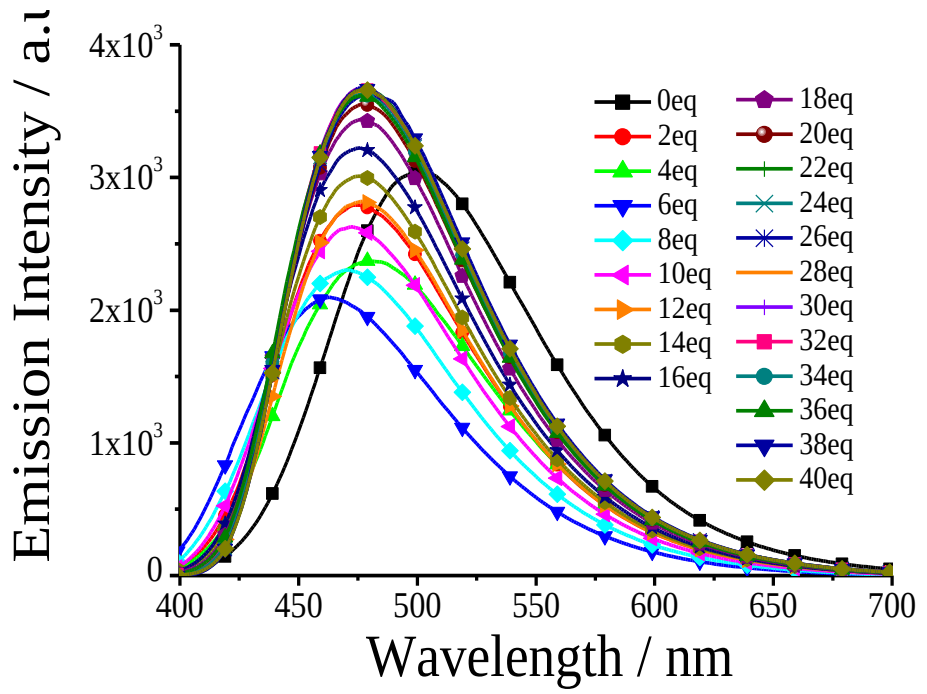

Fig. S32 Emission spectra of **(*R*,*R*)-3-Cl** with 20 equivalents of OH^- (1.0 × 10^{-5} mol dm^{-3} in EtOH, excited at 370 nm) upon the addition of different equivalents of Mg^{2+}.

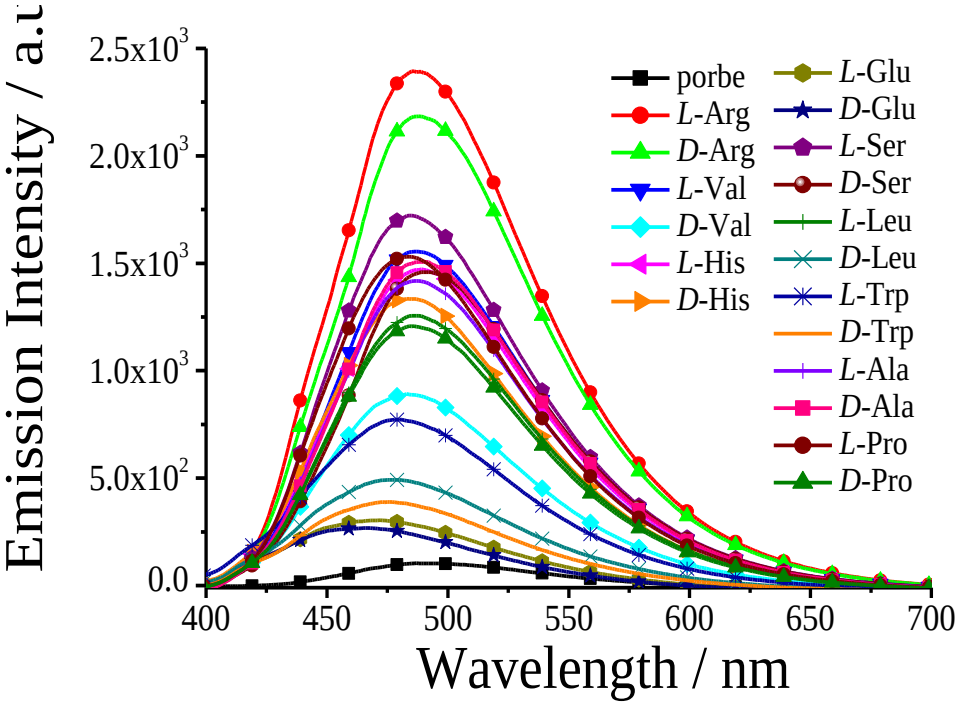

Fig. S33 Emission spectra of **(*R*,*R*)-3,5-Cl** (1.0×10^{-5} mol dm^{-3} in DMSO, excited at 390 nm) upon the addition of different 100 equivalents of amino acids.

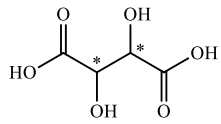

L/*D*-tartaric acid

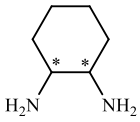

(*S*,*S*)/(*R*,*R*)1,2-Diaminocyclohexane
(*S*,*S*)/(*R*,*R*)DACH

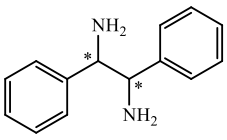

(*S*,*S*)/(*R*,*R*)1,2-Diphenyl-1,2-ethanediamine
(*S*,*S*)/(*R*,*R*)DPEDA

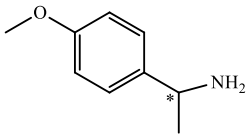

(*S*)/(*R*)1-(4-Methoxyphenyl)Ethylamine
(*S*)/(*R*)MEA

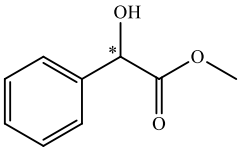

(*S*)/(*R*)Methyl mandelate
(*S*)/(*R*)MM

Fig. S34 Chemical strictures of selected chiral molecules.

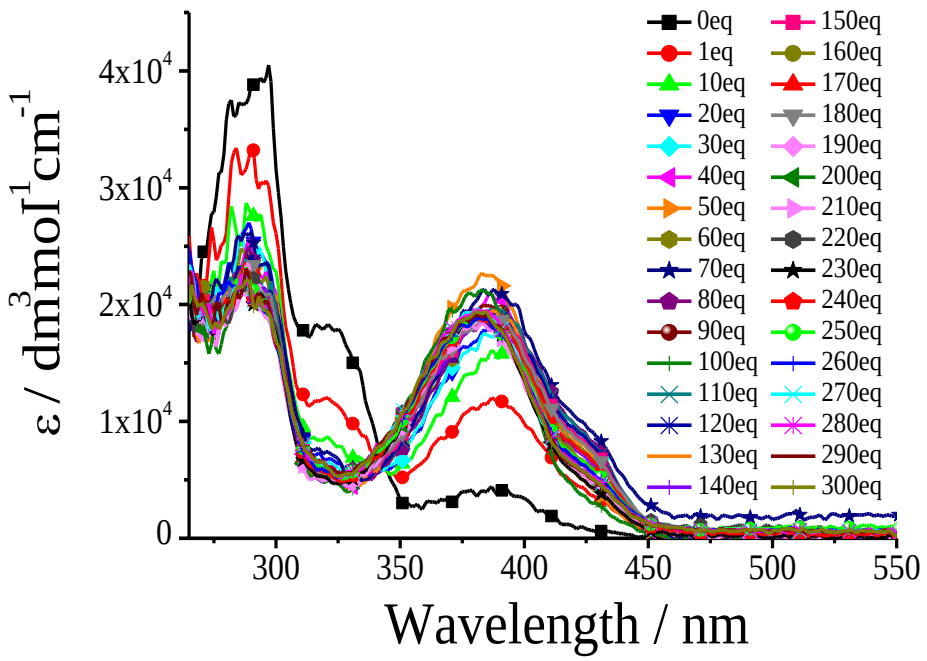

Fig. S35 Absorption spectra of **(*R*,*R*)-3-Cl** (1.0×10^{-5} mol dm^{-3} in DMSO) upon the addition of different equivalents of (*R*,*R*)-DACH.

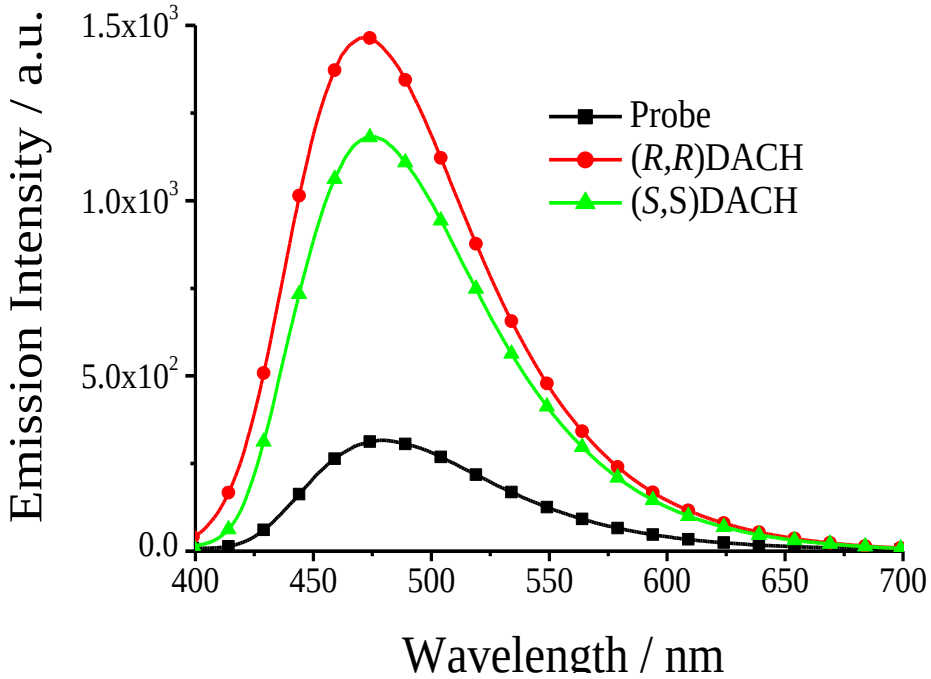

Fig. S36 Emission spectra of **(*R*,*R*)-3-Cl** (1.0×10^{-5} mol /dm^{-3} in DMSO, excited at 370 nm) upon the addition of different 100 equivalents of (*S*,*S*)/(*R*,*R*)DACH.

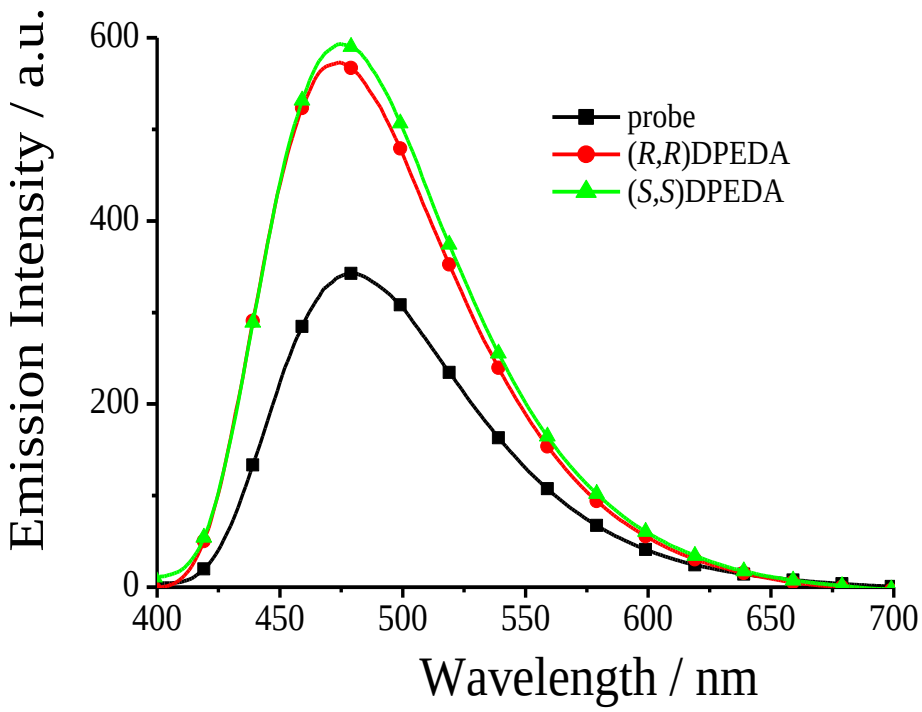

Fig. S37 Emission spectra of **(*R*,*R*)-3-Cl** (1.0 × 10^{-5} mol /dm^{-3} in DMSO, excited at 370 nm) upon the addition of different 100 equivalents of (*S*,*S*)/(*R*,*R*)DPEDA.

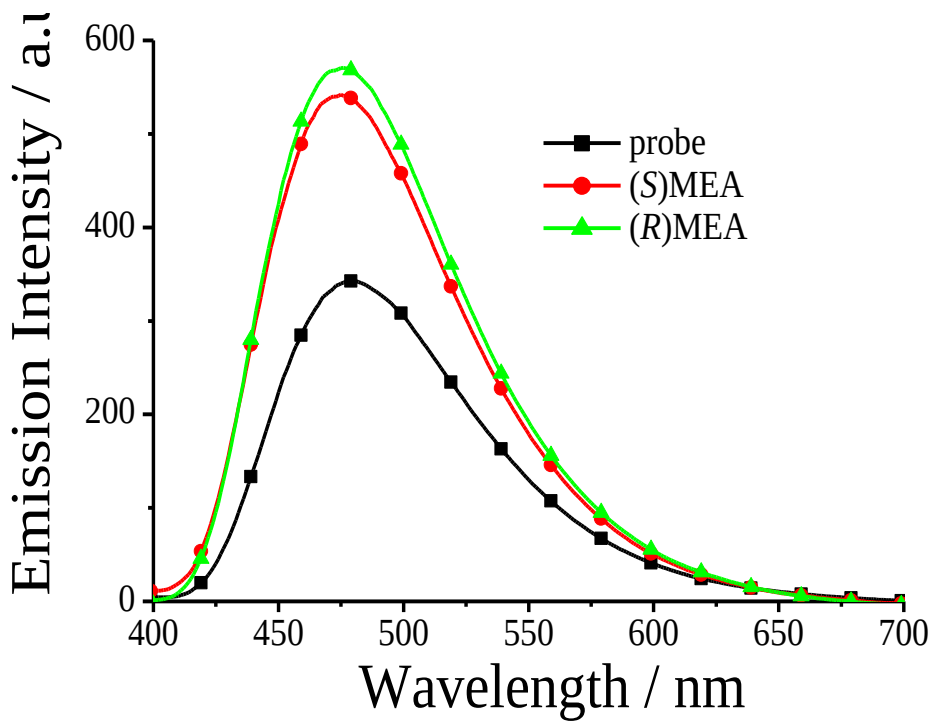

Fig. S38 Emission spectra of **(*R*,*R*)-3-Cl** (1.0 × 10^{-5} mol /dm^{-3} in DMSO, excited at 370 nm) upon the addition of different 100 equivalents of (*S*)/(*R*)MEA.

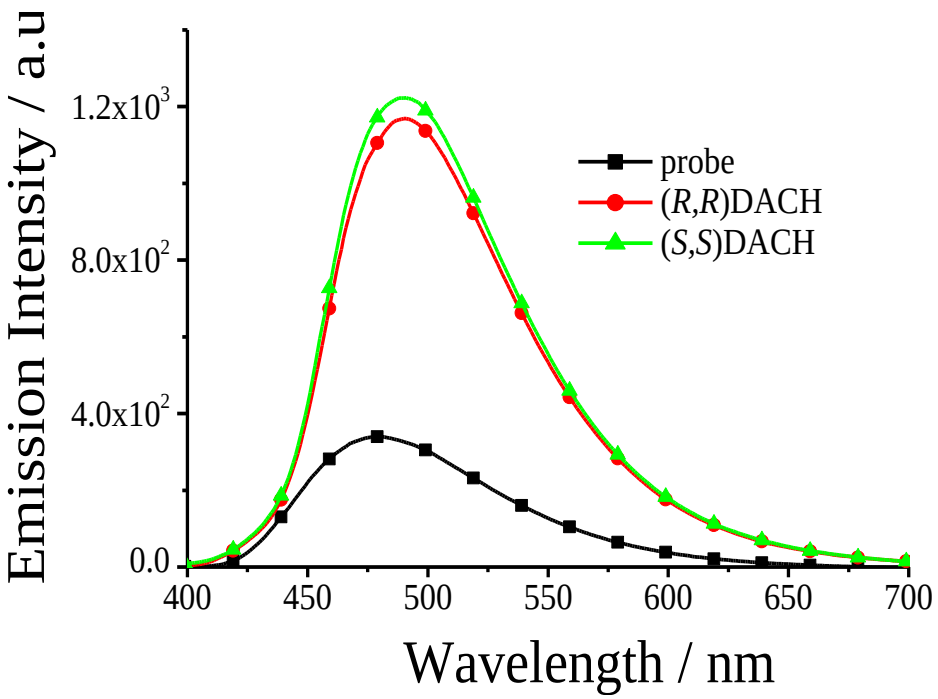

Fig. S39 Emission spectra of **(*S*,*S*)-3-Cl** (1.0×10^{-5} mol /dm^{-3} in DMSO, excited at 370 nm) upon the addition of different 100 equivalents of (*S*,*S*)/(*R*,*R*)DACH.

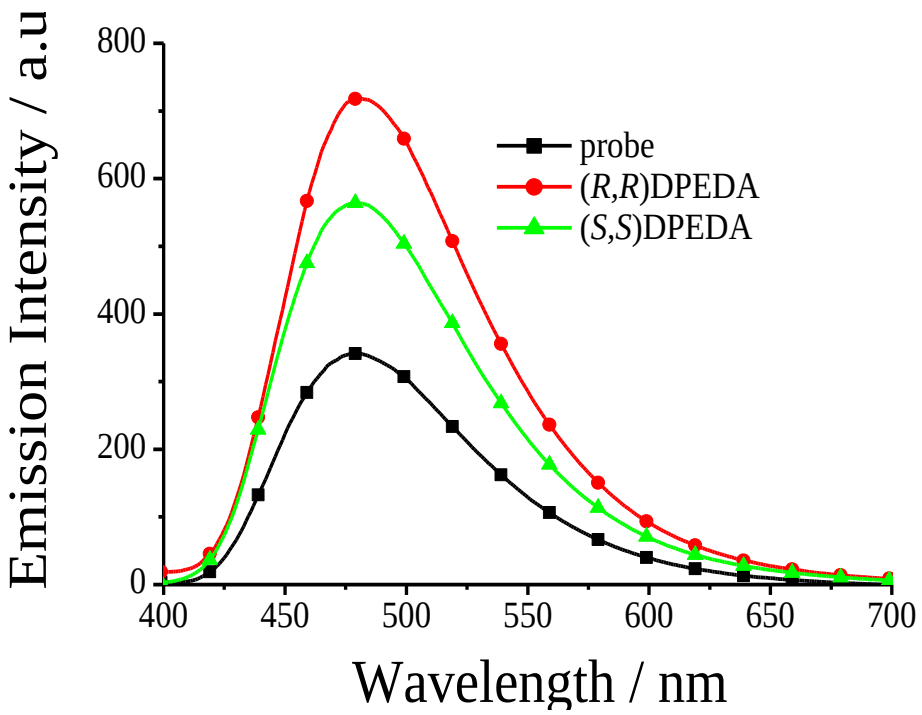

Fig. S40 Emission spectra of **(*S*,*S*)-3-Cl** (1.0×10^{-5} mol /dm^{-3} in DMSO, excited at 370 nm) upon the addition of different 100 equivalents of (*S*,*S*)/(*R*,*R*)DPEDA.

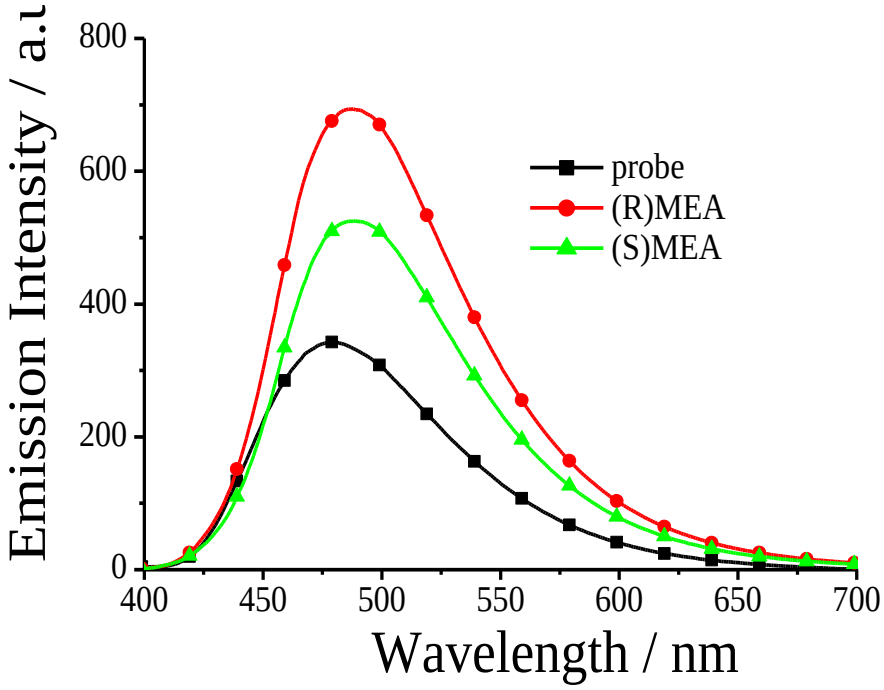

Fig. S41 Emission spectra of **(*S*,*S*)-3-Cl** (1.0×10^{-5} mol /dm^{-3} in DMSO, excited at 370 nm) upon the addition of different 100 equivalents of (*S*)/(*R*)MEA.

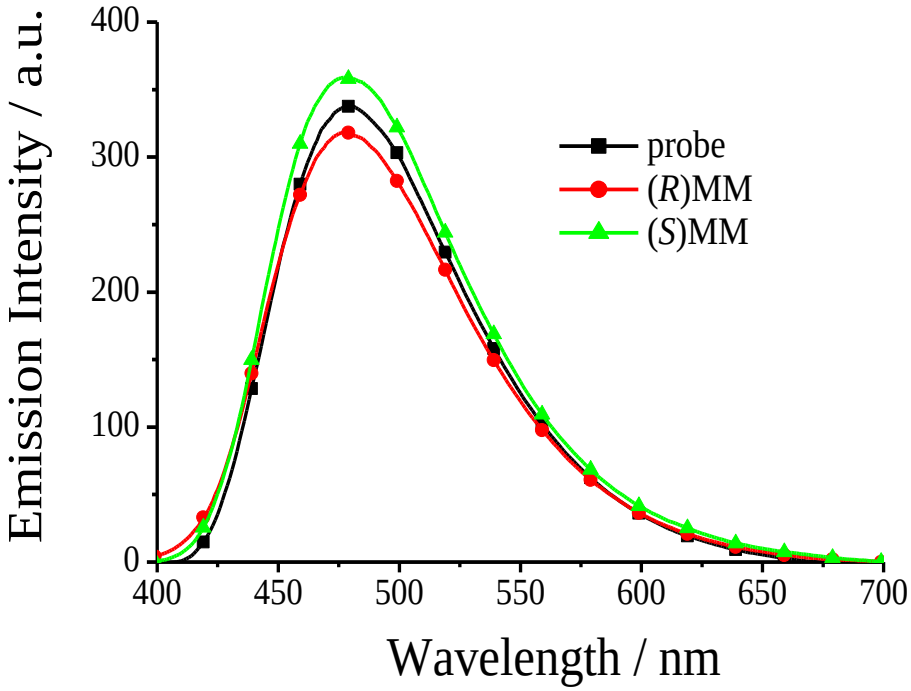

Fig. S42 Emission spectra of **(*S*,*S*)-3-Cl** (1.0×10^{-5} mol /dm^{-3} in DMSO, excited at 370 nm) upon the addition of different 100 equivalents of (*S*)/(*R*)MM.

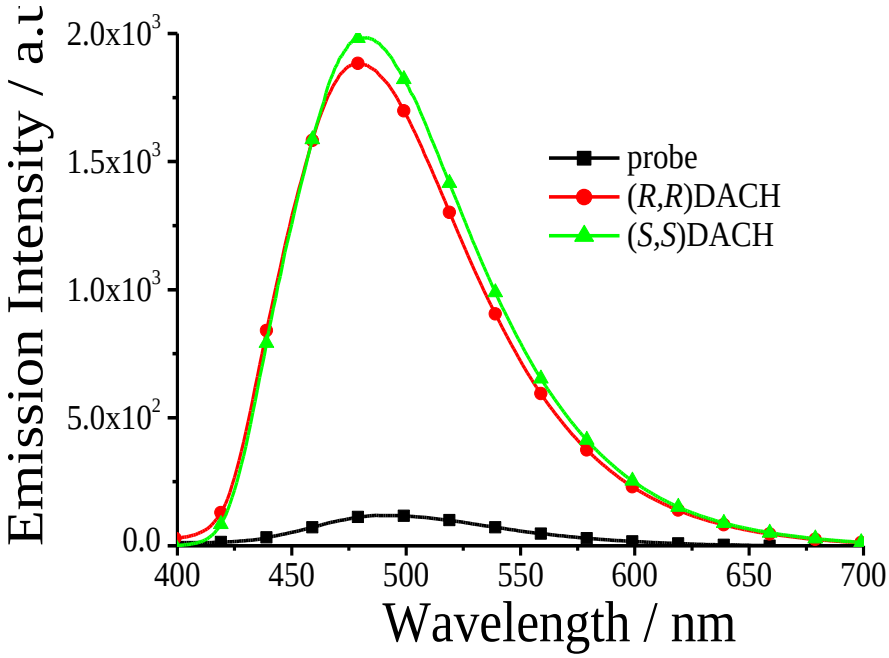

Fig. S43 Emission spectra of **(*S*,*S*)-3,5-Cl** (1.0×10^{-5} mol /dm^{-3} in DMSO, excited at 370 nm) upon the addition of different 100 equivalents of (*S*,*S*)/(*R*,*R*)DACH.

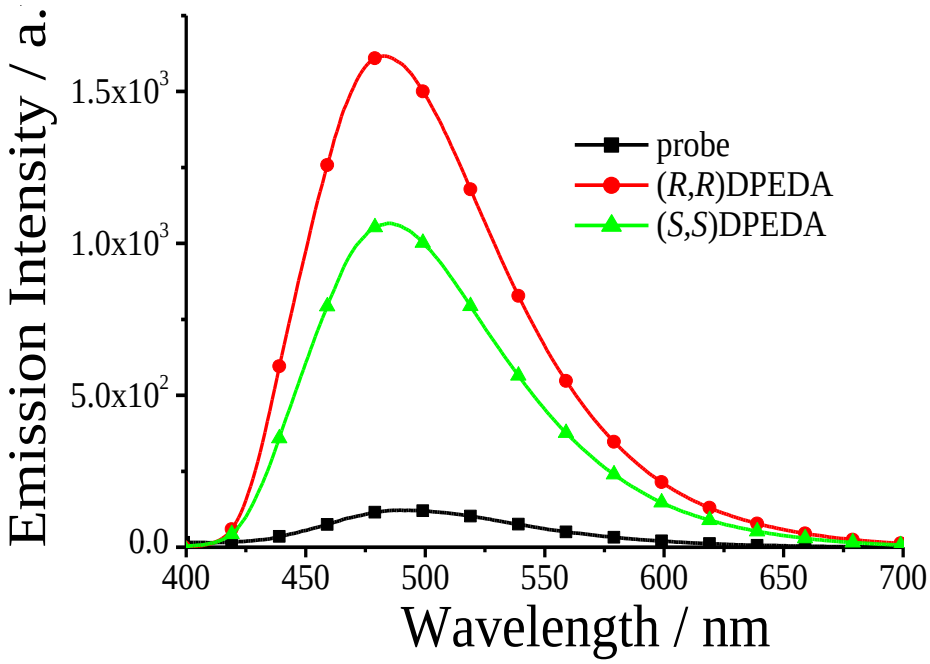

Fig. S44 Emission spectra of **(*S*,*S*)-3,5-Cl** (1.0×10^{-5} mol /dm^{-3} in DMSO, excited at 370 nm) upon the addition of different 100 equivalents of (*S*,*S*)/(*R*,*R*)DPEDA.

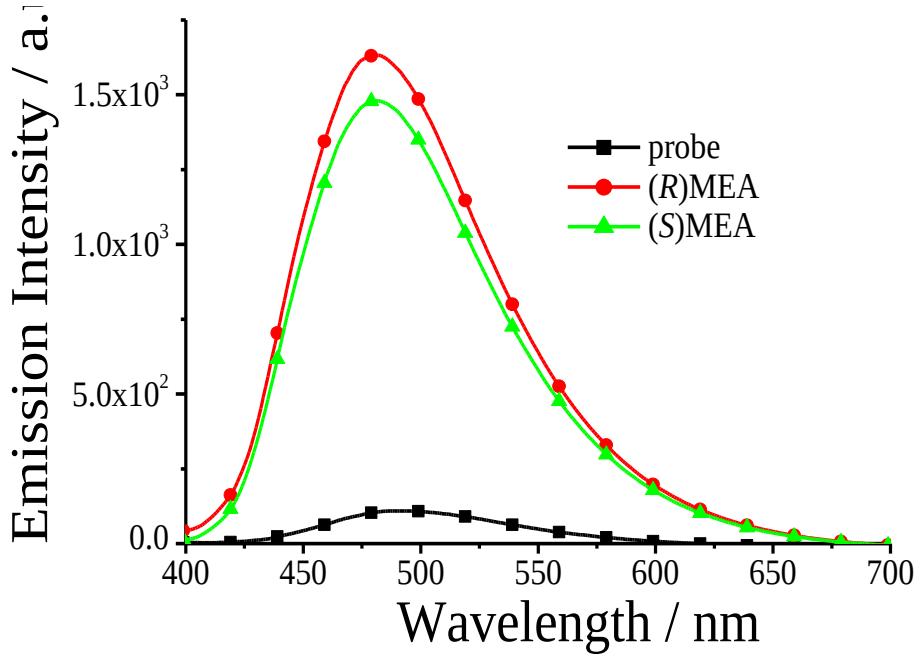

Fig. S45 Emission spectra of **(*S*,*S*)-3,5-Cl** (1.0 × 10^{-5} mol /dm^{-3} in DMSO, excited at 370 nm) upon the addition of different 100 equivalents of (*S*)/(*R*)MEA.

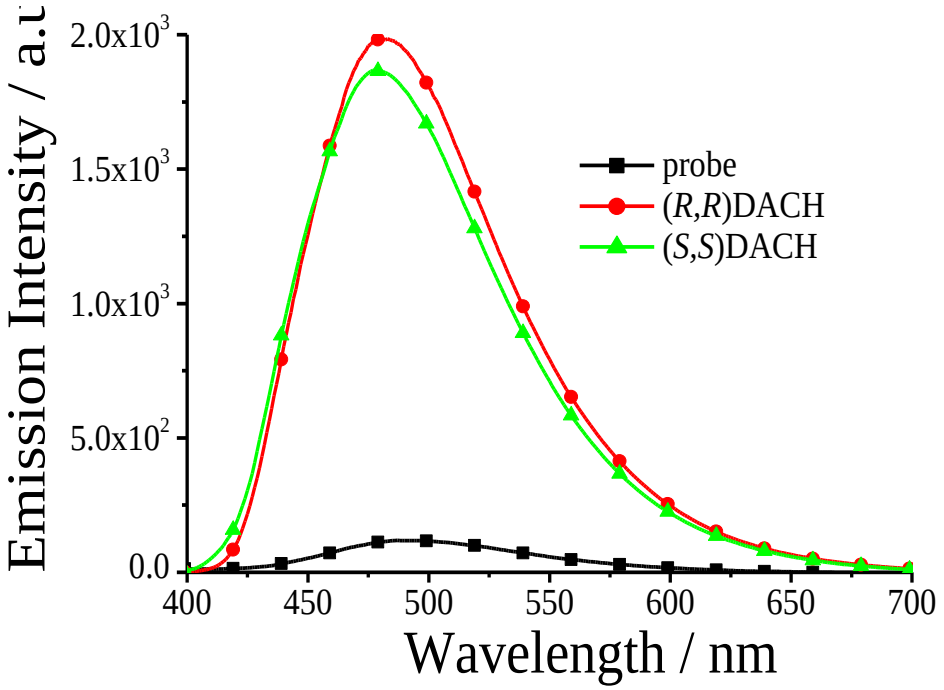

Fig. S46 Emission spectra of **(*R*,*R*)-3,5-Cl** (1.0 × 10^{-5} mol /dm^{-3} in DMSO, excited at 370 nm) upon the addition of different 100 equivalents of (*S*,*S*)/(*R*,*R*)DACH.

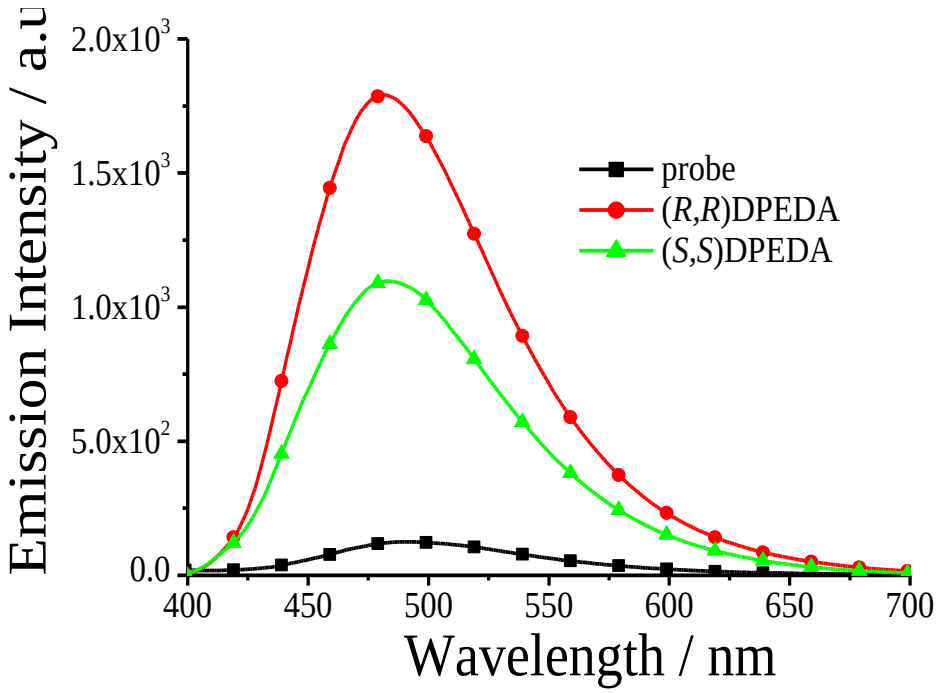

Fig. S47 Emission spectra of **(*R*,*R*)-3,5-Cl** (1.0×10^{-5} mol /dm^{-3} in DMSO, excited at 370 nm) upon the addition of different 100 equivalents of (*S*,*S*)/(*R*,*R*)DPEDA.

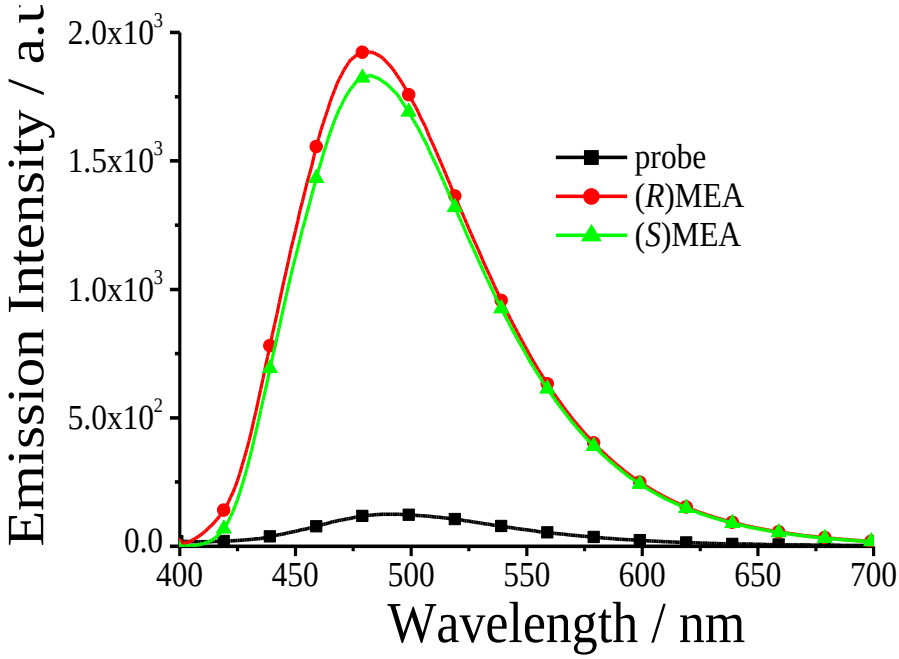

Fig. S48 Emission spectra of **(*R*,*R*)-3,5-Cl** (1.0×10^{-5} mol /dm^{-3} in DMSO, excited at 370 nm)upon the addition of different 100 equivalents of (*S*)/(*R*)MEA.

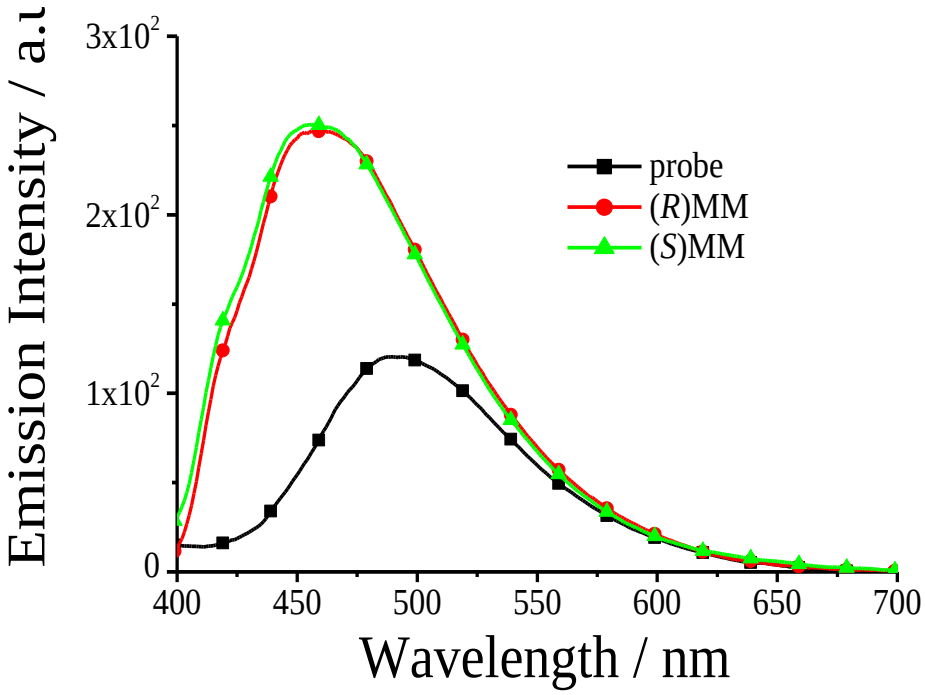

Fig. S49 Emission spectra of **(*R*,*R*)-3,5-Cl** (1.0×10^{-5} mol /dm^{-3} in DMSO, excited at 370 nm) upon the addition of different 100 equivalents of (*S*)/(*R*)MM.

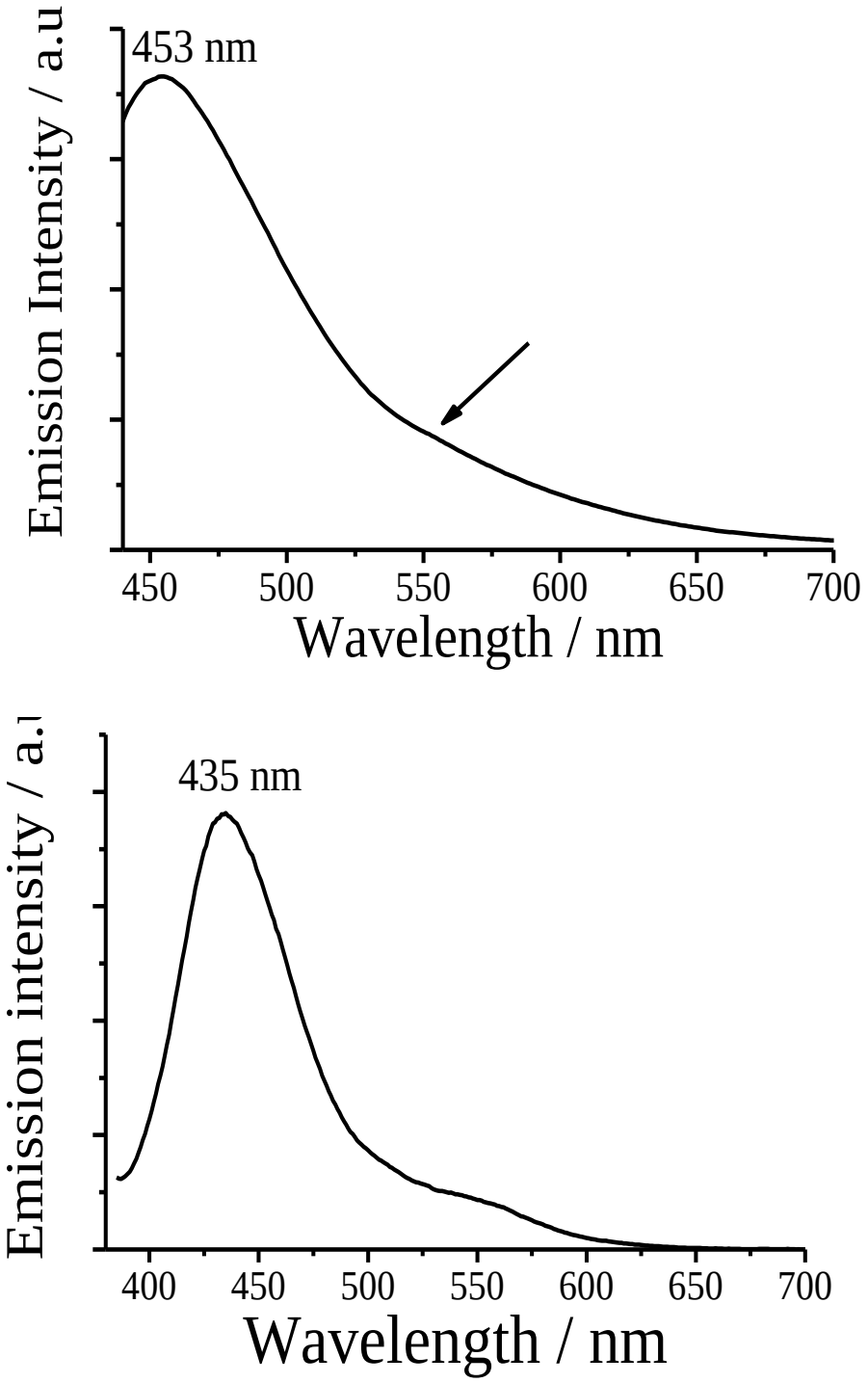

Fig. S50 Emission spectra of **(*R*,*R*)-3-Cl** (excited at 370 nm, 77 K) in 1.0 × 10^{-4} (top) and 5.0 × 10^{-4} (bottom) mol dm^{-3} EtOH.

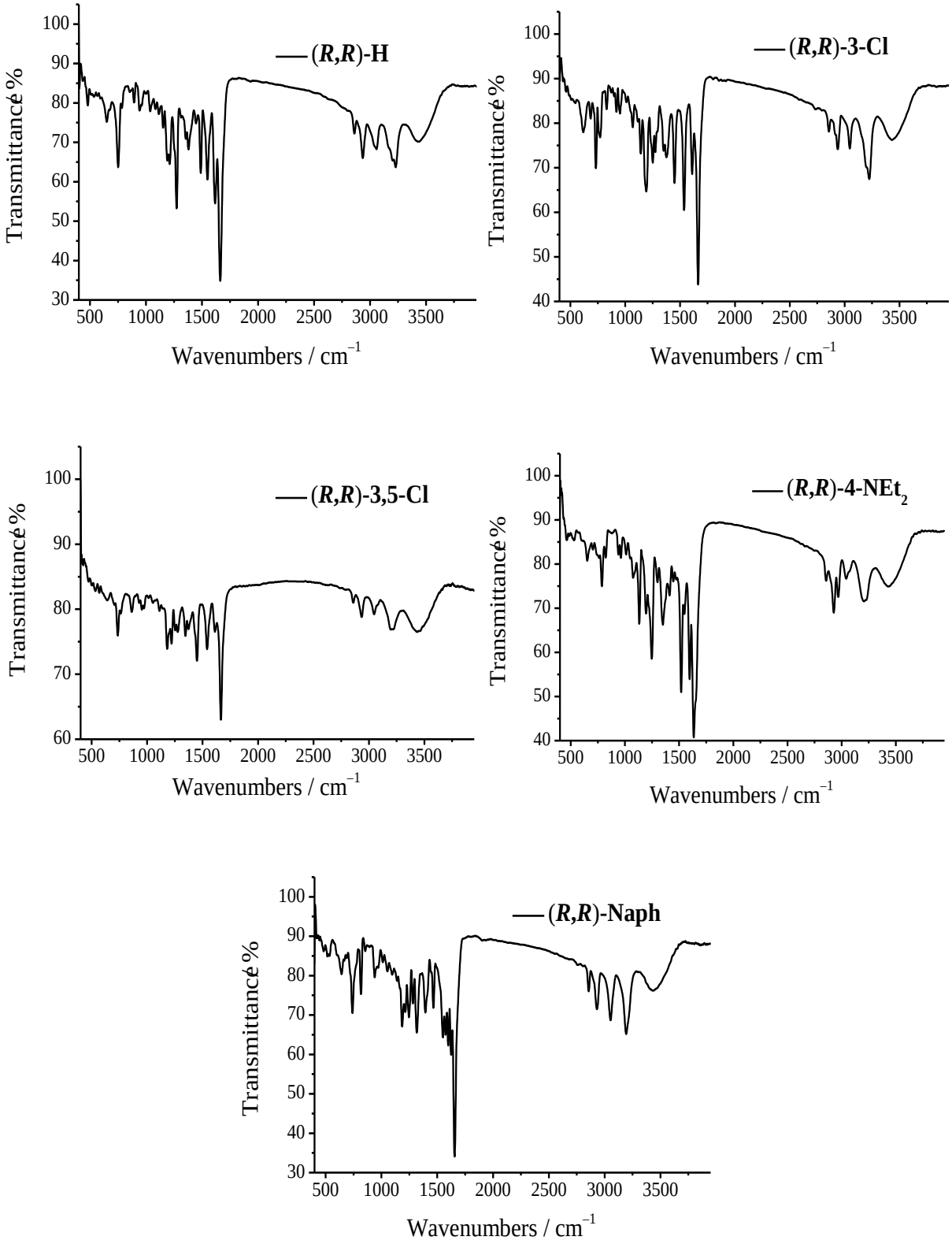

Fig. S51 IR spectrum of solid-state dyes.